Surface effects in non-linear distributed systems: slow relaxation and spontaneous emergence of localized coherent modes

Francesco Piazza
Laboratoire de Biophysique Statistique, ITP-SB
Ecole Politechnique Federale de Lausanne
CH-1015 Lausanne, Switzerland
Francesco.Piazza@epfl.ch

Contents

Abstract

As a general fact, spatially extended systems interact with the environment through their boundaries - for example when a flow of energy is established towards the exterior across the surface layers. When systems are characterized by sizeable surface fractions, as it is the case in the realm of meso-scopic or nano-scopic materials, this may lead to complex relaxation behaviours, such as non-exponential decay of macroscopic observables. What is even more interesting, the interplay of non-linearity and inhomogeneity of coupling to the environment in a relaxation process turns out to be a powerful way to drive a system into a region of its phase space characterized by meta-stable, long-lived localized solutions.

The interesting phenomenology begins with the simplest of all models, namely a system of beads connected by harmonic springs at equilibrium subjected to linear energy damping at its boundaries. I will review the rich analytical solution of this apparently trivial problem, showing how the system develops under those conditions an extended spectrum of relaxation rates causing the total energy to undergo a cross-over from an exponential to a power law, whose exponent depends on the spatial dimension. These results can be easily extended to elastic networks with arbitrary topology and also generalized to the case of stochastic relaxation to a given temperature.

In the second part of this paper, I will review the results of similar experiments performed on a selection of non-linear distributed systems: the 1D and 2D Fermi-Pasta-Ulam (FPU) lattices and the rotor chain. Although qualitatively different, edge relaxation in these systems inevitably results in the spontaneous formation of peculiar localized structures. These are meta-stable solutions of different nature that are practically decoupled from the boundaries, and thus display virtually infinite life-times. For example, in the FPU chain the relaxation process turns out to excite localized vibrating modes utterly analogous to a class of solutions of the corresponding Hamiltonian lattice known as discrete breathers. What is important, I will show how the spontaneous localization of energy can affect in a subtle way the transient time course of macroscopic observables, such as the total energy decay, before the pseudo-stationary state is attained. As a striking example of that, I will discuss some recent results of energy relaxation in a nonlinear network model of proteins, where the presence of spatial disorder adds non-trivial features to the spontaneous creation of localized vibrations.

In summary, besides the interest in its rich phenomenology per se, the process of edge cooling can thus be regarded as a natural way to direct a given system towards special regions of its phase space. These may be thought of as corresponding to low-complexity, quasi-periodic orbits that are "typical" in a loose sense. In this sense, such setting might be able to offer the exciting possibility to control the realization of selected coherent states.

1 Introduction

The usual way to look at vibrations in solids or molecules is to treat them as "bulk" properties. That is, the coupling with the environment of the system is either considered negligible (solids), or affecting all the atoms in the same way (molecules). While in the first case we usually deal with undamped modes of vibrations, in the latter class of systems we might neglect altogether the specificity of mode relaxation rates. In other words, we treat surface

effects in a "binary" fashion, either by completely neglecting them (solids have virtually zero surface fraction) or including them on all atoms equally (in molecules the surface fraction is virtually close to unity). However, there is a wide class of systems that sit in between such limiting cases: not so big as to make the all–bulk assumption entirely justifiable, nor so little that the difference between the bulk and surface domains might be sensibly ignored. These systems are characterized by linear sizes of the order of tens or hundreds of nanometers, and are thus often termed *nano-systems*.

In the last two decades, knowledge and technology have advanced tremendously in the multi-faceted realm of nano-science. Indeed, matter displays strikingly unusual properties when it is reduced in small objects of the size of the nanometer [1,2], so that the sometimes called nano-world appears to comprise domains as diverse as nano-electronics and the study of biochemical molecular motors at work in living cells. The interest in such fields of research has now pushed so deep that one of the major challenges is presently the design and construction of artificial nano-machines, i.e. macro-molecules and molecular assemblies, with directed or programmable internal dynamics [3]. As a consequence, it appears very important to understand the peculiar features of vibrational dynamics of systems on the nanometer scale.

A very rich and interesting phenomenology arises when surface effects are included in simple models of vibrational dynamics as a modelization of the interaction of the system with the environment [4]. The simplest example illustrating the rationale behind such models is the study of molecular motors [5–8]. Proteins, in fact, live immersed in a solvent and their dynamics is strongly damped as a result of the interaction of surface amino-acids with the external layers of waters composing the protein hydration shell. One interesting general point concerns relaxation to equilibrium of local or distributed energy fluctuations, such as may arise in enzimes as a result of ligand binding or more in general for the release of energy stored upon interaction e.g. with laser light. In living matter, it is long known experimentally that protein's responses may be highly non–exponential [9]. Recently, heat relaxation experiments in metallic nanoclusters have revealed that this is also the case in the realm of solid state nano–physics [10].

When non-linearity is also taken into account, the phenomenology gets surprisingly richer. In particular, it has been shown that surface effects such as edge damping result in spontaneous localization of energy in the form of long-lived, coherent vibrational modes [11]. These intrinsic localized vibrations are reminiscent of a class of spatially localized, time–periodic solutions, termed discrete breathers, recently discovered and characterized in a wide range of non-linear distributed systems [12–14]. At variance with their counterparts in the continuum, they exist under very general conditions and their existence and stability properties have been thoroughly investigated and rigorously assessed [15–17]. In particular, these objects may easily self–excite under very different physical conditions, as exemplified by several numerical and experimental studies [13, 18–23].

Quite generally, it seems that by virtue of surface effects it might be possible to excite *typical* localized coherent modes in a wide class of non-linear systems. This conjecture is beautifully exemplified by recent simulations of an optically confined Bose-Einstein con-

densate (BEC), where nonlinear self-trapped matter waves emerge spontaneously due to dissipative cooling applied at the lattice ends [24]. What is more important, the pseudo-stationary state obtained from the spontaneous localization process is within numerical error indistinguishable from an exact localized solution of the corresponding Hamiltonian problem. If these result are confirmed in other systems, edge cooling may become an extremely easy and efficient method capable of exploiting the spontaneous energy fluctuations of a given system in order to select in a natural fashion a "typical" exact localized solution. The perspectives opened by such considerations are very exciting.

The interplay of surface and non-linear effects may result in the emergence of complex behaviours even in systems as simple as one-dimensional chains of beads and springs [25–27]. In this paper, I will review the basic ideas underlying the mechanisms of slow-relaxation and spontaneous energy localization in a choice of linear and non-linear distributed systems in contact with the environment through the surface. I will start by discussing a simple but extremely informative example, namely a linear array of masses connected by harmonic springs in contact with a thermal bath at its edges. I will show how the inhomogeneity of coupling to the environment results in the emergence of a relaxation spectrum, whereby each Fourier mode relaxes exponentially with a different rate. As a consequence, the time relaxation of global observables becomes a sum of exponential processes that eventually originate power-law tails in the long-time limit. Moreover, I will demonstrate how, in the presence of spatial disorder, the superposition of exponential processes may result in a stretched exponential decay. To this regard I will introduce and discuss three-dimensional elastic network models and apply them to the study of relaxation in a globular protein and in a model nano-particle.

The example from the harmonic world will serve as a paradigm for rationalizing the results obtained when non-linearity enters the game. In this case, the behaviour of global observables is also strongly influenced by the details of the non-linear localized modes that spontaneously self-excite as a result of the surface damping. Depending on the class of non-linear systems examined, the overall relaxation behaviour may then be the expression of sheer non-linear effects or still bear the character of the surface damping. It is important to state this point in a clear fashion, because the lack of a thorough understanding on how to properly disentangle the two mechanisms may lead to entirely wrong interpretations. Finally, I will discuss the role of coupling spatial disorder to nonlinearity by discussing the spontaneous localization process in a dimer protein (Citrate Synthase) modeled as a three-dimensional network of FPU springs.

2 Relaxation in harmonic systems

When they first discovered the phenomenon of spontaneous localization upon edge cooling in a linear chain with non-linear on-site potential in 1996 [11], Serge Aubry and George Tsironis commented: "When the system temperature is reduced further, the breather size increases, and they quickly disappear from the picture; the energy relaxation is now completely phonon dominated since at small temperatures only the linear part of the potential is

effective and thus energy relaxation proceeds in the usual exponential fashion." Breathers indeed disappear from the picture, but in fact the system cannot recover its usual exponential relaxation, since this is not what happens in a harmonic lattice damped at its edges. The reason why Aubry and Tsironis got it wrong in this otherwise inspiring piece of work is that they did not wait long enough. In fact, as I will show in the first part of this paper, a linear system whose energy is being extracted from its boundaries only relaxes exponentially on a time scale of order N. After that a crossover to an inverse-power law sets in, thus slowing down the energy decay independently of the formation of localized structures.

Surprisingly enough, many authors since fell in the same trap, by taking for granted that a linear system under such conditions should relax exponentially. This equivocation in turn led to further subsequent misunderstandings, in the quest for stretched exponential decays in other systems as well (see for example the paper [28] then updated and revised in [29]). It is thus worthwhile to discuss here the behaviour of harmonic systems in the first place, before moving on to the phenomenon of spontaneous energy localization.

2.1 The harmonic chain

In this section, I illustrate the solution of a seemingly simple exercise, namely a chain of N equal masses connected by springs of equal strength, coupled to a heat bath at its edges. The chain is first prepared in an equilibrium state and we want to compute the total energy during the transient as time flows since the edge thermostats are switched on.

We consider a chain that at $t = 0$ is at equilibrium at a temperature T_0. Modeling the system à la Langevin, only the first and last particles are damped and subject to randomly fluctuating forces due to their interaction with the solvent, according to the equations

$$\begin{aligned} m\ddot{u}_p &= V'(u_{p+1} - u_p) - V'(u_p - u_{p-1}) \quad p = 2, 3, \ldots, N-1 \\ m\ddot{u}_1 &= V'(u_2 - u_1) - m\zeta\dot{u}_1 + \xi_1 \\ m\ddot{u}_N &= -V'(u_N - u_{N-1}) - m\zeta\dot{u}_N + \xi_N \end{aligned} \tag{1}$$

where $V(x) = kx^2/2$ is the inter-particle potential, u_p and and $\xi_p(t)$ ($p = 1, 2, \ldots, N$) are the particle displacements and random forces, respectively, and ζ is the viscous friction coefficient. As we are dealing with a system in a finite volume, we will impose either free ($u_{-1} = u_0$, $u_{N-1} = u_N$) or fixed-ends ($u_{-1} = u_N = 0$) boundary conditions (BC). The random forces model a Gaussian, delta-correlated white noise, whose standard deviation is fixed by the fluctuation dissipation theorem

$$\langle \xi_p(t)\xi_{p'}(t')\rangle = 2k_B T m\zeta\, \delta_{p,p'}\delta(t - t') \quad .$$

We want to investigate how the system relaxes to a temperature $T < T_0$. In particular, we want to determine the law describing the decay of global observables such as the total energy.

The time behavior of the system only depends on the temperature difference $\Delta T = T_0 - T$ because of the absence of local energy barriers in the energy landscape. This property

can be proved rigorously by solving the Fokker–Planck (FP) equation associated with the Langevin equations (1) [4] (see subsection 2.3). As a consequence, we may solve the ($T_0 \rightarrow T$) stochastic problem as that of a deterministic dissipative system of energy $Nk_B\Delta T$ which is only damped at its edges. The exact solution of this problem is most easily obtained by rewriting the equation of motion in matrix form. With zero fluctuating forces we have

$$\dot{U} = \mathbb{A}\, U, \tag{2}$$

where $U = (u_1, \ldots, u_N, \dot{u}_1, \ldots, \dot{u}_N)^T$ is a $2N$ column vector, and $\mathbb{A}$ is the matrix

$$\mathbb{A} = \left(\begin{array}{c:c} 0 & \mathbb{I}_N \\ \hdashline K & -\Gamma \end{array} \right) \quad . \tag{3}$$

Here we use reduced units, whereby times are rescaled by a factor $\omega_0 = \sqrt{k/m}$. Hence, the tri–diagonal matrix of force constants is given by

$$K_{ij} = \delta_{i,j+1} + \delta_{i,j-1} - 2\delta_{i,j} \quad 1 < i, j < N$$

and also contains the information on the type of boundary conditions, whereas the matrix

$$\Gamma_{ij} = \eta\delta_{i,j}(\delta_{j,1} + \delta_{j,N})$$

describes the coupling with the environment. Herafter, we indicate with

$$\eta = \frac{\zeta}{\omega_0}$$

the *reduced* friction coefficient. The solution of Eq. (3) can be written as

$$U(t) = e^{\mathbb{A}t}U(0) = \left[\Psi_R\, e^{\Lambda t}\, \Psi_L^T\right] U(0)$$

where $\Lambda_{ij} = \lambda_i\delta_{ij}$ is the diagonal matrix of the eigenvalues of $\mathbb{A}$, and Ψ_R and Ψ_L are the matrices of right and left eigenvectors, respectively. The spectrum of damping rates and modified frequencies is hence obtained by diagonalizing matrix $\mathbb{A}$. In Fig. 1 we plot $\gamma(\omega)$ for different values of the damping strength η, where $\gamma_i = -\Re(\lambda_i)$ and $\omega_i = \Im(\lambda_i)$ for the i-th eigenvalue. It is apparent that, for $\eta \geq 1$ (i.e. the usual critical point of half the band-edge frequency), the zero–frequency mode acquires an additional real eigenvalue that in the overdamped regime becomes equal to the damping strength η (see also panel (d) in Fig. 1). This behaviour is illustrated in Fig. 2, where the maximum and second largest damping rates are plotted as functions of η. In particular, we see that in the underdamped regime $\gamma_0 \simeq 2\eta/N$, whereas in the overdamped regime $\gamma_0 = \eta$ while the second largest rate $\gamma_1 \simeq 2/\eta N$ (we recall that damping rates are here measured in units of ω_0). Hence, the maximum of the extended band of damping rates grows proportionally to the damping strength in the underdamped regime, whereas it is inversely proportional to it in the overdamped regime.

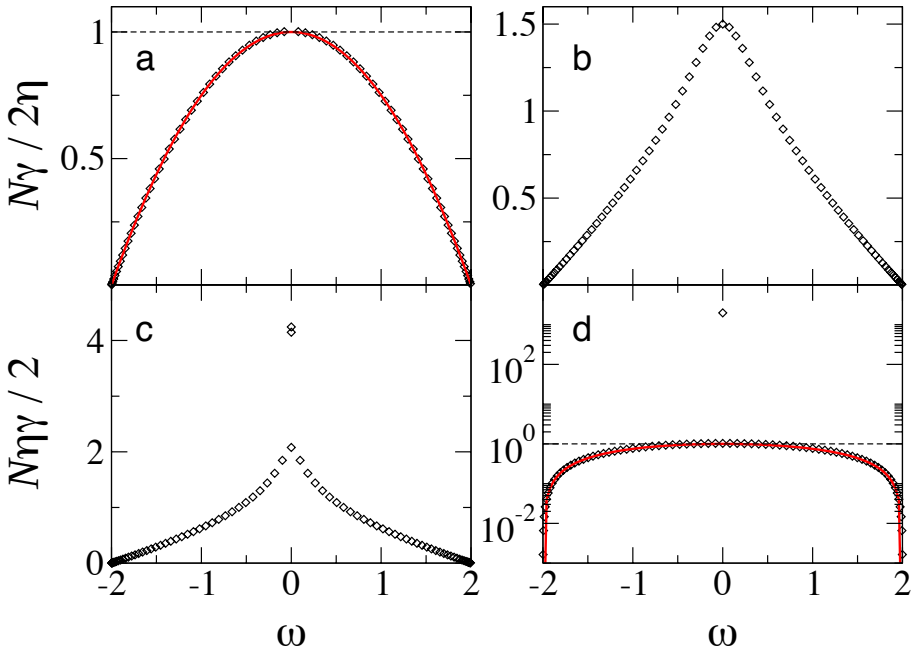

Figure 1: Spectrum of damping rates $\gamma(\omega)$ for an harmonic chain with free ends and $N = 40$ and $\eta = 0.1$ (a), $\eta = 0.9$ (b), $\eta = 1.1$ (c), $\eta = 10$ (d). The solid lines in panels (a) and (d) are plots of the analytical perturbative approximations (8).

In the underdamped $(\eta \ll 1)$ and overdamped $(\eta \gg 1)$ regimes the relaxation spectrum can be calculated analytically by means of perturbation theory. Let $-\omega_\alpha^2$ and ψ^α $(\alpha = 0, 1, \ldots N-1)$ denote the eigenvalues and normalized eigenvectors, respectively, of the unperturbed hamiltonian problem, where

$$\omega_\alpha^2 = 4\,\sin^2\left(\frac{q_\alpha}{2}\right) \quad . \tag{4}$$

and we have introduced the wave–numbers $q_\alpha = \alpha\pi/N$ (free ends) and $q_\alpha = (\alpha+1)\pi/N$ (fixed ends). For $(\eta \ll 1)$ we may look for solutions of the form

$$u_n(t) = \sum_{\alpha=0}^{N-1} c_\alpha(t) e^{-i\omega_\alpha t}\psi_n^\alpha. \tag{5}$$

where ψ_n^α is the n-th component of the eigenvector ψ^α. By substituting expression (5) in the equations of motion (2), we can rewrite them in the form of a system of differential equations for the c_α's. We can then find approximate solutions by expressing the latter as power series in the non-dimensional perturbation parameter η. The details of the calculation are reported in Appendix A. To first order in η we obtain

$$c_\alpha(t) = c_\alpha(0) e^{-\gamma_\alpha t} \tag{6}$$

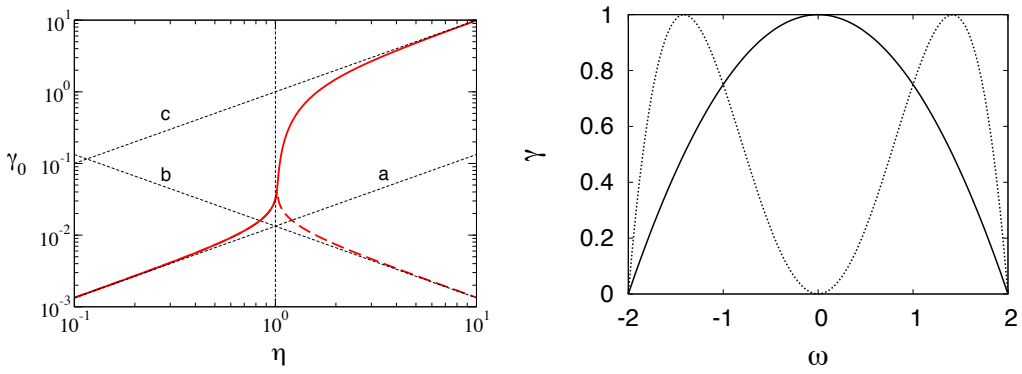

Figure 2: (a) Plot of the first and second largest damping rates of the relaxation spectrum in a chain with free ends as functions of the reduced damping strength η. The two rates coincide for $\eta \leq 1$ whereas they progressively detach from one another for $\eta > 1$. The dashed lines represent the asymptotic trends. (a) Straight line $\gamma_0 = 2\eta/N$; (b) plot of the law $\gamma_0 = 2/N\eta$; (c) straight line $\gamma_0 = \eta$. Here $N = 150$. (b) Plot of the relaxation spectra (8) for a free-ends (solid line) and a fixed-ends (dotted line) harmonic chain with surface damping.

where

$$\begin{aligned} \gamma_\alpha &= \gamma_0 \cos^2\left(\frac{q_\alpha}{2}\right) \quad \ldots \quad \text{Free ends BC} \\ \gamma_\alpha &= \gamma_0 \sin^2\left(q_\alpha\right) \quad \ldots \quad \text{Fixed ends BC} \quad . \end{aligned} \tag{7}$$

We recall that in the underdamped regime $\gamma_0 = 2\eta/N$, whereas in the overdamped regime $\gamma_0 = 2/\eta N$ (see again Fig. 2). Finally, by recalling the expression of the linear spectrum Eq. (4) and dropping the mode index α, Eqs. (7) may be rewritten in the more concise form

$$\begin{aligned} \gamma(\omega) &= \gamma_0 \left(1 - \frac{\omega^2}{4}\right) \quad \ldots \quad \text{Free ends BC} \\ \gamma(\omega) &= \gamma_0 \left(\frac{\omega^2}{4}\right)\left(1 - \frac{\omega^2}{4}\right) \quad \ldots \quad \text{Fixed ends BC} \end{aligned} \tag{8}$$

with

$$\gamma_0 = \begin{cases} f\eta & \eta \ll 1 \\ \dfrac{f}{\eta} & \eta \gg 1 \end{cases}$$

Note that we have explicitly introduced in the last expressions the *surface* fraction $f = 2/N$.

The relaxation spectra (8) are drawn in Fig. 2 (b). It is evident that the type of boundary conditions does make a large difference. In the case of free ends, the least damped modes are the short–wavelength ones, the largest lifetime being $1/\gamma_N \approx 2N^3/\pi^2\eta$, while the most damped modes are the ones in the vicinity of $\omega = 0$, with $1/\gamma_0$ being the shortest decay time. In a chain with fixed ends, the picture changes dramatically. From one side, band-edge modes show to be more damped with respect to the case of free ends. Secondly, the

low-frequency modes show in this case to be as little damped as the latter ones. This is an important observation. We shall comment further on this result later on in the paper, as it proves to be very important in the case of relaxation under the same conditions in non-linear lattices. In fact, for certain non-linear potentials, a mechanism intriguingly similar to modulational instability of short-wavelength waves [30] is observed to guide the system toward energy localization as a direct result of the longer persistence of the latter modes in the lattice [31].

We have found that a system coupled to the environment through its surface acquires an extended spectrum of relaxation rates. One that may even span several orders of magnitude, depending on the choice of the parameters (see again panel (d) of Fig. 1). As a consequence, in such framework the decay process of a given global observable will be the superposition of N exponential processes. However, the fastest one has a decay rate that is proportional to the surface fraction of the system. Thus, in general, we can imagine that the first stage of the relaxation process will be single-exponential with a decay constant that depends on how much the system topology exposes it to the environment. After that stage, all modes will take over and the decay will slow down onto a superposition of exponentials. In particular, it is reasonable to think that the time scale for such crossover be $\tau_0 = 1/\gamma_0 \propto 1/f$. If this is the case, the less the system is exposed to the environment the longer its exponential relaxation, whereas systems with greater surface fractions will sooner show a slow down of the relaxation kinetics. We are now in a position to investigate analytically the above conjecture. For such purpose, we shall compute the behaviour of the total energy decay.

2.1.1 The energy decay

The system energy E is defined as $E = \sum_p e_p$, where we have introduced the so–called symmetrized site energies

$$e_p \;=\; \frac{1}{2} m \dot{u}_p^2 + \frac{1}{2}\left[V(u_{p+1} - u_p) + V(u_p - u_{p-1})\right].$$

Using the above definition of the system energy and the solution (6), we can explicitely evaluate the normalized energy as

$$\frac{E(t)}{E(0)} = \frac{\sum_\alpha c_\alpha^2(0)\,\omega_\alpha^2\, e^{-2\gamma_\alpha t}}{\sum_\alpha c_\alpha^2(0)\,\omega_\alpha^2}. \tag{9}$$

As we are interested in the typical behaviour of the system when it evolves from equilibrium initial conditions, we replace $c_\alpha^2(0)\omega_\alpha^2$ with its average value $2E(0)/N$. Thus, recalling expressions (7) and approximating for large N the sum over α with an integral, we have

$$\frac{E(t)}{E(0)} = \frac{1}{\pi}\int_0^\pi e^{-2\gamma(q)t}\, dq = e^{-\frac{t}{\tau_0}} I_0\left(\frac{t}{\tau_0}\right) \tag{10}$$

where I_0 is the modified zero–order Bessel function. It is important to stress that the choice of the boundary conditions turns out to be irrelevant for the *integrated* behaviour of the energy decay. The asymptotic behaviour of the function (10) in fact evidentiates that a crossover exists on the time scale $1/\gamma_0 \propto 1/f$. We have

$$\frac{E(t)}{E(0)} = \begin{cases} e^{-t/\tau_0} & \text{for } t \ll \tau_0, \\ \dfrac{1}{\sqrt{2\pi(t/\tau_0)}} & \text{for } t \gg \tau_0. \end{cases} \tag{11}$$

Hence, in the case of a harmonic chain the energy decay crosses over to an inverse-power law with exponent $1/2$. In fact, this result may be easily generalized to dimension d and one finds that the exponent of the power law is $d/2$. This result suggests that the energy, after a first exponential relaxation stage dominated by the fraction of actively relaxing particles, starts *diffusing* away. However, the system contains a finite number of particles, and consequently a finite number of modes. This means that, when the energy stored in all modes will have drained away, there will be only the slowest mode with significant energy left. As a result, the energy decay will again speed up to an exponential law of the type $\exp(-2t/\tau_{N-1})$, with $\tau_{N-1} \propto N^3$. Therefore, the time extent of decay region dominated by the inverse-power law increases as N^3 for large values of the system size.

The time scale for the onset of the slowing down of the energy flow is inversely proportional to the surface fraction f. Hence, this effect should disappear in the thermodynamic limit, where $f \propto N^{-1/d} \to 0$, d being the spatial dimension. However, besides mesoscopic and nano-scopic materials where surface effects are fundamental [1], there are other contexts where it makes little sense to use the thermodynamic limit, such as in the presence of long-range forces [32]. Hence, the role of surface effects in the exchange of energy between a body and the enviroment or between two bodies may not be trivial in many cases. In this respect, it is instructive to discuss an analogy in the continuum of the problem of a hot harmonic chain of particles that relaxes to a smaller temperature.

2.2 The continuum analogy

It is interesting to formulate a macroscopic analogy of the problem of edge relaxation in a one-dimensional system in the form of a boundary problem for the heat equation in $1D$. The initial condition would be a piecewise constant profile of the type

$$T(x,0) = \begin{cases} T_i & \text{for} \quad |x| < \ell \qquad \text{(region 1)} \\ T_f & \text{for} \quad |x| > \ell \qquad \text{(region 2)} \end{cases} \tag{12}$$

with $T_i > T_f$. The problem may be solved in full generality by assigning to the two regions different thermal properties, i.e. introducing two steady-state thermal conductivities κ_r and two thermal diffusion coefficients D_r, $r = 1, 2$. It is then possible to solve the boundary problem and calculate the reduced average temperatures as functions of time, i.e.

$$\langle \Theta_r(t) \rangle = \frac{\langle T_r(t) \rangle - T_f}{\Delta T} \tag{13}$$

where $\Delta T = T_i - T_f$ and

$$\begin{aligned} \langle T_1(t)\rangle &= \frac{1}{\ell}\int_0^{\ell} T_1(x,t)\,dx \\ \langle T_2(t)\rangle &= \lim_{L\to\infty}\frac{1}{L-\ell}\int_{\ell}^{L} T_2(x,t)\,dx \end{aligned} \tag{14}$$

The details of the calculations are given in Appendix B. The result for the decay of the energy stored initially in region 1 reads

$$\langle \Theta_1(t)\rangle = \frac{2\,\mathbb{K}}{\pi}\int_0^{\infty} e^{-u^2(t/\tau_1)}\left(\frac{\sin u}{u}\right)^2 \frac{du}{\mathbb{K}^2\cos^2 u + \sin^2 u} \tag{15}$$

where $\tau_1 = \ell^2/D_1$ and $\mathbb{K}$ is the relative heat strength parameter, defined as

$$\mathbb{K} = \frac{\kappa_2}{\kappa_1}\sqrt{\frac{D_1}{D_2}} \tag{16}$$

The diffusivity is a measure of how quickly a body can change its temperature, and it characterizes transient heat transfer problems, whereas the thermal conductivity describes thermal steady-state processes. We can eliminate the thermal conductivities in expression (16) by recalling the definition of the thermal diffusion coefficient in terms of the heat capacity C_p and density ρ of the medium

$$D = \frac{\kappa}{C_p\rho} \quad .$$

thus obtaining

$$\mathbb{K} = \frac{C_{p,2}\,\rho_2}{C_{p,1}\,\rho_1}\sqrt{\frac{D_2}{D_1}} \tag{17}$$

It is therefore clear that the parameter $\mathbb{K}$ is a measure of the relative ability of the two media to conduct heat in a transient process.

It is not difficult to realize that the asymptotic behaviour of the solution (15) for $t \gg \tau_1$ is (see Appendix B)

$$\langle \Theta_1(t)\rangle \sim \frac{1}{\mathbb{K}}\sqrt{\frac{\tau_1}{\pi t}} \quad . \tag{18}$$

Hence, the $t^{-1/2}$ decay is recovered in one-dimension in the continuum approximation of the energy flow as heat diffusion. The same calculation may be repeated in higher dimension d to confirm that heat asymptotically *diffuses* away from the initial hot region with exponent $d/2$ [33].

It is interesting to note that in the continuum approximation the temperature decay of the initially hot region also displays a crossover from an exponential law to the power law $t^{-d/2}$. However, at variance with the discrete case, the initial exponential regime in the

continuum is a *stretched* one, of the type $\langle\Theta_1(t)\rangle \propto \exp[-(t/\tau_1)^\sigma]$ with $\sigma = 1/2$. This is most easily seen when medium 1 and 2 are the same. In this case, one has $\mathbb{K} = 1$ and hence

$$\langle\Theta_1(t)\rangle = \frac{2}{\pi}\int_0^\infty e^{-u^2(t/\tau_1)}\left(\frac{\sin u}{u}\right)^2 du \quad . \tag{19}$$

The integral (19) can be computed analytically by noticing that

$$\frac{\partial\langle\Theta_1(t)\rangle}{\partial t} = -\frac{2}{\pi\tau_1}\int_0^\infty e^{-u^2(t/\tau_1)}\sin^2 u\, du = -\frac{1}{2\sqrt{\pi\tau_1 t}}\left(1 - e^{-\tau_1/t}\right) \quad . \tag{20}$$

By integrating Eq. (20) with the asymptotic condition $\lim_{t\to\infty}\langle\Theta_1(t)\rangle = 0$, we finally get

$$\langle\Theta_1(t)\rangle = \mathrm{erf}\left(\sqrt{\frac{\tau_1}{t}}\right) - \sqrt{\frac{t}{\pi\tau_1}}\left(1 - e^{-\tau_1/t}\right) = \begin{cases} e^{-\sqrt{t/\pi\tau_1}} & \text{for } t \ll \tau_1 \\ \sqrt{\frac{\tau_1}{\pi t}} & \text{for } t \gg \tau_1 \end{cases} \quad . \tag{21}$$

In the general case $\mathbb{K} \neq 1$, Eq. (15) tells us that the time scale of the stretched exponential $\rightarrow$ inverse-power law crossover is set by the thermal and physical properties of the two media as

$$\tau_{\text{eff}} = \frac{\tau_1}{\mathbb{K}^2} \propto \frac{1}{D_2} \tag{22}$$

By looking at expression (22) one may realize that, when the two media are characterized by very different heat conduction properties ($\mathbb{K} \ll$ or $\gg 1$), the crossover may shift to very early to vary late times, thus pushing the asymptotic inverse-power law regime in a region of undetectable temperature variations. In particular, if medium 2 is much less thermally conducive than medium 1, one has $\tau_{\text{eff}} \gg \tau_1$, i.e. the characteristic time for establishing a power law decay is much longer than the typical time scale of heat diffusion over a length ℓ. In this case, $\mathbb{K} \ll 1$ and the temperature decay will be dominated by the initial stretched exponential law. On the contrary, if medium 2 is much more thermally conducive than medium 1, an efficient heat transfer may be established at the boundary since the thermal reservoirs are well conducive. As a consequence, $\tau_{\text{eff}} \ll \tau_1$ ($\mathbb{K} \gg 1$) and the diffusive regime may be rapidly established. However, τ_{eff} also represents the time constant of the initial exponential decay. Therefore, in the former case, where it takes long to establish the power law regime, the temperature drop reached at the crossover time will be small. As a consequence, the power-law regime will be detectable by waiting enough. We may thus think at the environment as a *viscous* medium, characterized by a high thermal resistivity. On the contrary, in the case where the diffusive regime is readily established, the temperature drops considerably during the stretched exponential stage, thus making the power law regime hardly detectable. These considerations are illustrated in Fig. 3.

2.3 Relaxation in higher-dimensional elastic networks

We have seen that surface effects in elastic lattices cause each linear mode to relax exponentially with a prescribed rate. Consequently, energy extraction through the boundaries

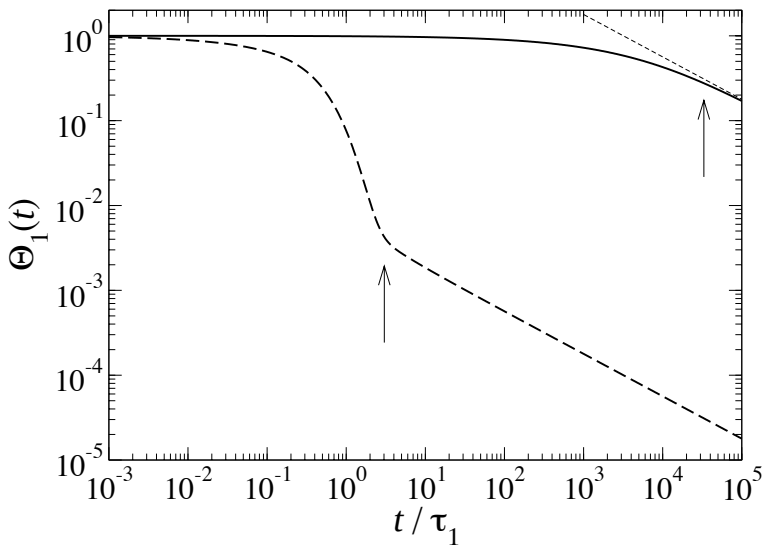

Figure 3: Decay of the average normalized temperature of the initially hot region (medium 1) calculated by numerical computation of the integral (15). Solid line $\mathbb{K} = 0.1$. Dashed line $\mathbb{K} = 100$. The arrows indicate the crossover to the asymptotic power law relaxation (18) (explicitly shown as the thin dashed line in the case $\mathbb{K} = 0.1$)

in dimension d, eventually lead to a crossover to an inverse-power law with exponent $d/2$, whose rationale can be found in the theory of heat diffusion. In this section we show how the same formalism can be generalized to arbitrary three-dimensional networks of harmonic springs and arbitrary values of the equilibrium temperature through the Fokker-Planck (FP) formalism. The dynamics of the system which has undergone a local or distributed energy fluctuation will be modeled through a system of Langevin equations. Starting from such formulation, the corresponding FP equations will be introduced and solved for arbitrary initial conditions. It is important to stress that the type of framework considered here applies to the case where the relaxation is slow with respect to the characteristic time of rearrangement of the particles that constitute the thermal bath. In this sense, the relaxation pathway proceeds adiabatically from an equilibrium states to another in such a way that the solvent has efficiently rearranged its configuration much faster compared to the changes occurred in the system.

2.3.1 The Elastic Network Formalism

The simplest way to study the vibrational properties of an object of nano-scopic dimensions such as a protein, a piece of double stranded DNA helix or a metal nano-particle is to model the structure as a collection of point particles with given masses connected by harmonic springs [34–38]. This type of modeling may also imply some coarse-graining of the structures, whereby group of selected atoms are grouped together in a fictitious point particle with mass equal to the total mass of the group and equilibrium position lying at its centre of

mass. In these coarse-grained models $\vec{r}_i$ represents the position of the effective point particle, $\vec{r}_{i0}$ its equilibrium position. In the case of a biological macromolecule that would be the native state (proteins) as determined from X-ray crystallography or Nuclear Magnetic Resonance, or any other equivalent experimental determination of a stable structure.

The total potential energy of the system is a sum of pairwise harmonic potentials

$$U(\{\vec{r}_i\}) = \frac{1}{2}\sum_{i,j} V(\vec{r}_i, \vec{r}_j) = \frac{1}{2}\sum_{i,j} \frac{k_{ij}}{2}(|\vec{r}_i - \vec{r}_j| - |\vec{r}_{i0} - \vec{r}_{j0}|)^2 \tag{23}$$

where k_{ij} is the interaction stiffness between particles i and j. The force constants k_{ij} can take different functional forms, such as

$$k_{ij} = k\ \theta(r_c - |\vec{r}_{i0} - \vec{r}_{j0}|) \tag{24}$$

($\theta(x)$ being the Heaviside step function) or

$$k_{ij} = k\ \exp(-|\vec{r}_{i0} - \vec{r}_{j0}|^2/r_c^2) \quad . \tag{25}$$

In either case r_c is a suitable cutoff (or typical) interaction distance that tunes the overall connectivity of the structure, and k a phenomenological strength constant. The models based on the expression (24) are usually referred as *sharp cutoff* (SC) models, whereas those based on expression (25) are known as Gaussian elastic networks (GNM) models. It should be noted that there is no specific reason why a Gaussian decay should be chosen for the effective force constants. In fact, any other decreasing functions of the equilibrium particle inter-distance could be utilized as well.

In the harmonic approximation, the total potential energy (23) can be written as a quadratic form

$$U = \frac{1}{2}(X - X^0)^T K\,(X - X^0) \tag{26}$$

where $X = \{r_{1,x}, r_{1,y}, r_{1,z}, \ldots, r_{N,x}, r_{N,y}, r_{N,z}\}$ is the vector of particle positions, X^0 is the same vector corresponding to equilibrium positions and the "contact" matrix K is the Hessian matrix of the potential energy function evaluated at the equilibrium structure.

$$K_{i,j}^{\alpha,\beta} = \left(\frac{\partial U}{\partial r_{i,\alpha} r_{j,\beta}}\right)_{X=X^0} \quad . \tag{27}$$

The dynamics of the system immersed in a solvent at a temperature $\beta = 1/k_B T$ can be described by the following system of Langevin equations

$$m_i \ddot{r}_{i,\alpha} = \sum_{j=1}^{N}\sum_{\beta=1}^{3}\left[K_{i,j}^{\alpha,\beta}(r_{j,\beta} - r_{j,\beta}^0) - m_i \Gamma_{i,j}^{\alpha,\beta}\dot{r}_{j,\beta}\right] + R_{i,\alpha}(t) \quad i = 1, 2, \ldots, N\ \ \alpha = 1, 2, 3 \tag{28}$$

where Γ is the matrix of damping strenghts and $R_i(t)$ are random fluctuating forces satisfying the fluctuation-dissipation theorem

$$\begin{aligned} &\langle R_{i,\alpha}(t)\rangle = 0 \\ &\langle R_{i,\alpha}(t)R_{j,\beta}(t')\rangle = 2\beta^{-1}m_i\Gamma_{i,j}^{\alpha,\beta}\delta_{i,j}\delta_{\alpha,\beta}\delta(t-t') \quad . \end{aligned} \tag{29}$$

The central idea of our treatment is that the coupling with the solvent should be significant only for particles exposed on the surface of the system, whereas those lying in the bulk are shielded from these interactions. For the sake of simplicity, we neglect here hydrodynamic interactions between particles, which makes the matrix Γ diagonal[1]. Consequently, the latter has the form

$$\Gamma_{ij}^{\alpha,\beta} = \zeta\delta_{i,j}\delta_{\alpha,\beta}S_i \tag{30}$$

where the vector S specifies the fraction of surface exposed to the solvent by each particle ($0 < S_i < 1$, $i = 1, 2, \ldots, N$). The parameter ζ specifies a physical scale for the strength of the viscous force.

The problem described by the set of coupled stochastic ordinary differential equations (28) can be reformulated in terms of the associated Fokker-Planck equation for the corresponding probability density in phase space

$$\frac{\partial P(Y,t|Y(0))}{\partial t} = \sum_{i,j=1}^{6N}\left[-\mathbb{A}_{i,j}\frac{\partial}{\partial Y_i}Y_j + \mathbb{B}_{i,j}\frac{\partial^2}{\partial Y_i\partial Y_j}\right]P(Y,t|Y(0)) \tag{31}$$

where $Y = M^{1/2}(X - X^0, \dot{X})$ is the $6N$–dimensional vector of mass-weighted displacements and velocities with M the diagonal mass matrix. The matrices $\mathbb{A}$ and $\mathbb{B}$ are given by

$$\mathbb{A} = \left(\begin{array}{c:c} 0 & \mathbb{I}_{3N} \\ \hdashline -\mathbb{K} & -\mathbb{G} \end{array}\right) \qquad \mathbb{B} = \beta^{-1}\left(\begin{array}{c:c} 0 & 0 \\ \hdashline 0 & \mathbb{G} \end{array}\right) \quad . \tag{32}$$

where

$$\begin{aligned} \mathbb{G} &= M^{-1/2}\Gamma M^{-1/2} \\ \mathbb{K} &= M^{-1/2}KM^{-1/2} \quad . \end{aligned}$$

The solution of Eq. (31) is the multivariate Gaussian distribution [40]

$$\begin{aligned} P(Y,t|Y(0)) = (2\pi)^{-3N}|\det C(t)|^{-1/2}\times \\ \exp\left\{-\frac{1}{2}[Y - \mathcal{G}(t)Y(0)]^T C^{-1}(t)[Y - \mathcal{G}(t)Y(0)]\right\} \end{aligned} \tag{33}$$

[1]Hydrodynamic interactions occur when a particle partly shields another from the viscous effects of the solvent molecules [39]. However, in the context of a protein structure bulk particles are to a good extent *isolated* from the solvent, which prompts the idea that interactions with its neighbours should not include damping.

where $C_{i,j}(t) = \langle Y_i(t) Y_j(t) \rangle$ is the block correlation matrix

$$C = \left(\begin{array}{c:c} C_{XX} & C_{X\dot{X}} \\ \hdashline C_{X\dot{X}} & C_{\dot{X}\dot{X}} \end{array} \right) \tag{34}$$

and $\mathcal{G}(t)$ is the propagator matrix. The latter can be evaluated at any time in terms of the normalized bi-orthogonal set of left and right eigenvectors of the matrix $\mathbb{A}$, also known as Langevin modes

$$\mathcal{G}(t) = \Psi_R \, e^{\Lambda t} \, \Psi_L^T \tag{35}$$

where $\Lambda_{ij} = \lambda_i \delta_{ij}$ is the diagonal matrix of the eigenvalues of $\mathbb{A}$, and Ψ_R and Ψ_L are the matrices of right and left eigenvectors, respectively. It is easy to show that the evolution law for the correlations reads, in matrix form,

$$C(t) = C(\infty) + \mathcal{G}(t)[C(0) - C(\infty)]\mathcal{G}^T(t) \tag{36}$$

where we have introduced the equilibrium correlation matrix

$$C(\infty) = \beta^{-1} \left(\begin{array}{c:c} \mathbb{K}^{-1} & 0 \\ \hdashline 0 & \mathbb{I}_{3N} \end{array} \right) \tag{37}$$

Due to the invariance under rigid roto-translations of the system energy, the matrix $\mathbb{K}$ has 6 zero eigenvalues. Hence, the inverse $\mathbb{K}^{-1}$ is to be intended in the generalized sense

$$\mathbb{K}^{-1}_{ij} = \sum_{\alpha=1}^{3N-6} \frac{1}{\lambda_\alpha} \Psi^\alpha_{R,i} \Psi^\alpha_{L,j} \quad .$$

We are now in a position to calculate the energy relaxation to equilibrium of a given local or distributed energy excitation. We first diagonalize matrix $\mathbb{A}$ and then evaluate the correlation matrix (36) as a function of time with the aid of Eq. (35). The expression for the total energy then reads

$$\begin{aligned} \langle E(t) \rangle &= \langle T(t) \rangle + \langle U(t) \rangle \\ \langle T(t) \rangle &= \frac{1}{2} \mathrm{Tr} \, \left[C_{\dot{X}\dot{X}}(t) \right] \\ \langle U(t) \rangle &= \frac{1}{2} \mathrm{Tr} \, \left[\mathbb{K} C_{XX}(t) \right] \quad . \end{aligned} \tag{38}$$

In order to illustrate the above worked out formalism, I shall present the results of energy relaxation in Myoglobin, a globular protein, and in a simple icosahedral nano-particle [41]. In the case of Myoglobin, the elastic network is constructed by grouping all atoms of a given residue into a point particle which is assigned the total mass of the residue and whose equilibrium position is taken to coincide with that of the α-carbon, i.e. on the backbone

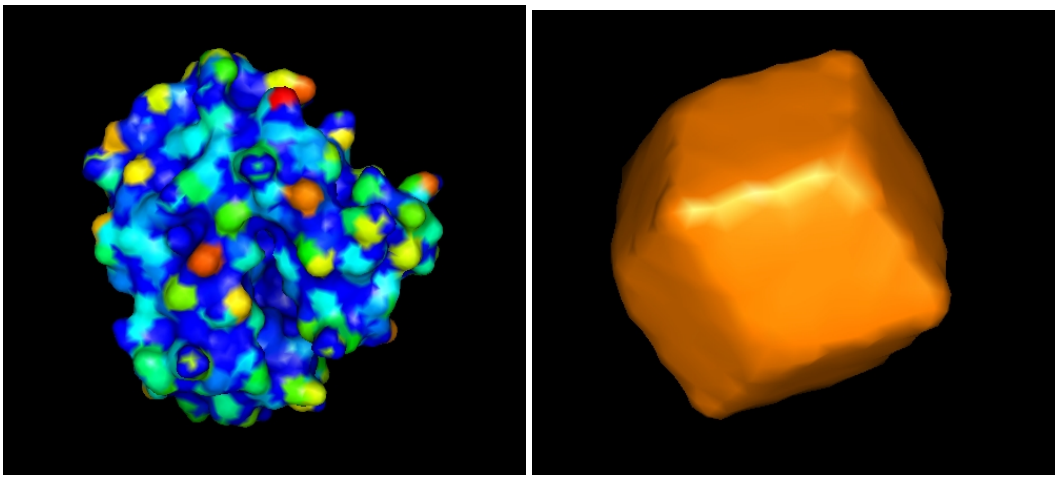

(a) (b)

Figure 4: Structure of Myoglobin (pdb code 1A6M) and of a model rhombic icosahedral metal cluster with $N = 335$ atoms. The protein structure is color–coded according to the fraction of surface accessible to the solvent at each site – from blue (low accessibility) to red (highest exposure).

chain. No coarse graining is peformed in the case of the metal nanocluster. The Myoglobin molecule has $N = 194$ residues, including the HEME group, and a linear size in the range $4 \div 5$ nm. The metal cluster considered here has $N = 335$ Au atoms, arranged in the bulk onto a simple cubic lattice with cell size $a = 2.9$ Å, which corresponds to a linear size of the aggregate of about 2.3 nm. The effective fraction of surface exposed to the solvent at each site (the vector S) is calculated through a standard solvent-accessible surface area (SASA) model [42] (see Fig. 4).

As the simplest example, I assume that the structures are prepared at equilibrium at a given temperature T_0 and examine how the energy is released along the relaxation pathway theat leads to equilibrium at temperature $T < T_0$. Consequently, the specific potential energy is initially set at its equilibrium value $3\beta^{-1}/2$, while each particle is given the kinetic energy $3\beta_0^{-1}/2$. This amounts to taking in Eq. (36)

$$C(0) = \left(\begin{array}{c:c} \beta^{-1}\mathbb{K}^{-1} & 0 \\ \hdashline 0 & \beta_0^{-1}\mathbb{I}_{3N} \end{array} \right) \tag{39}$$

Incidentally, the form of the latter assignment, together with Eq. (36), also prove that the relaxation process only depends on the temperature difference $\Delta T = T_0 - T$.

As a first example, I plot in Fig. 5 the decay of the average kinetic, potential and total energy per particle in the case of Myogobin both in the under-damped regime ($\zeta \ll \Im[\lambda_{3N-6}]$)

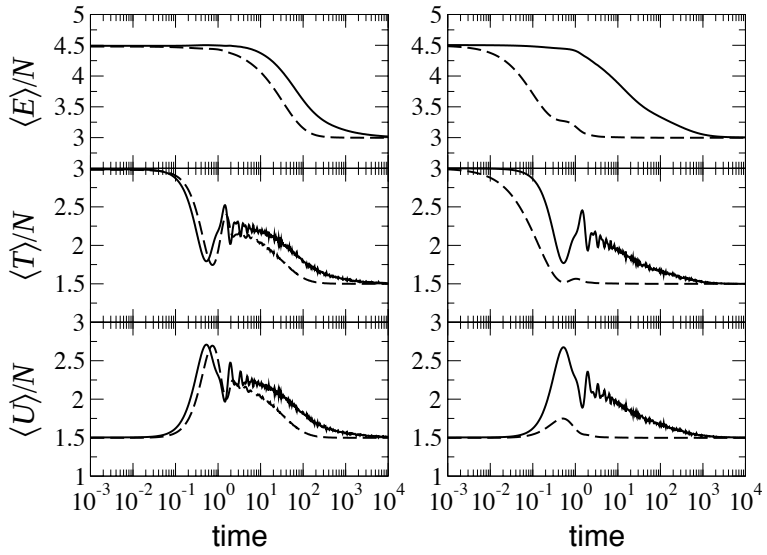

Figure 5: Average decay of surface (dashed line) and bulk (solid line) energies per particles in Myoglobin in the under-damped (left panels) and over-damped (right panels) regimes. The bulk is defined as the ensemble of all residues whose effective surface exposed to the solvent is smaller than 10 % of the highest exposed surface. This definition corresponds to a surface–to–volume ratio of about 0.56 which is about twice as much as the *true* surface fraction $f = \sum_i S_i \simeq 0.24$. Energies are measured in units of $k_B T$. Parameters are $T_0 = 2T$, $N = 151$, $m\zeta = 0.27$ ps^{-1} (left panels) and $m\zeta = 27$ ps^{-1} (right panels). The mass m has been taken equal to the average amino-acid mass $m \approx 2 \times 10^{-25}$ Kg.

and in the over-damped regime ($\zeta \gg \Im[\lambda_{3N-6}]$). A first observation confirms that the surface portion of the structure relaxes much faster in the over-damped regime. However, a less trivial fact also occurs - the relaxation of the energy initially stored in the bulk is much less affected by the increase of the damping rate at the surface and displays a relaxation that is only slightly faster with respect to the under-damped case. What happens is that a great deal of the energy initially deposited in the surface flows away very rapidly, leaving the bulk particles with a *mismatch* with the particles lying in the outer layer, which are soon emptied of their initial energy and keep henceforth oscillating with small amplitude.

The decay of the total energies follows a similar pathway in both structures (see Fig. 6). The first relaxation stage proceeds exponentially, each structure with a rate determined by its surface fraction. Remarkably, we see that the time constant for such exponential decay is nothing but $\tau_0 = 1/f\zeta$, i.e. an expression formally identical to that we have derived analytically in the case of the harmonic chain, whereby here the surface fraction f is generalized to (see Eq. (30))

$$f = \frac{1}{N} \sum_i S_i \tag{40}$$

Following the first stage, a crossover to a slower decay is observed in complete analogy

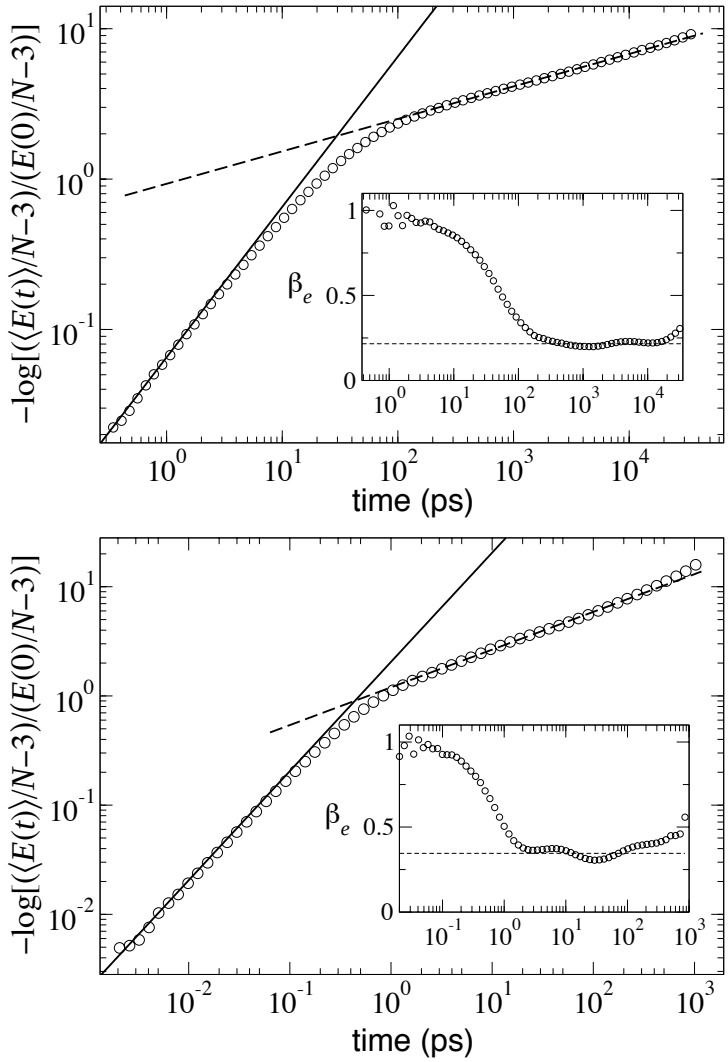

Figure 6: Relaxation of total energy to equilibrium in Myoglobin (a) and in an rhombic icosahedral Au cluster (b) as calculated through Eq. (38) in units of β^{-1} (symbols). The crossover from the initial exponential trend with time constant $\tau_0 = 1/f\zeta$ (solid lines) to a slower trend is evident. The latter is well fitted by a stretched exponential law of the type $\exp[-(t/\tau)^\sigma]$ with exponent $\sigma = 0.216$ (a) and $\sigma = 0.345$ (b) (dashed lines). The effective exponent β_e calculated from Eq. (41) is shown in the insets (symbols), along with the best fit value calculated after the crossover (dashed lines). Parameters are $T_0 = 2T$, $N = 194$, $f = 0.242$, $r_c = 8$ Å (a) and $N = 335$, $f = 0.48$, $r_c = 6$ Å (b). For calculating physical units in the case of Myoglobin, the mass m has been taken equal to the average amino-acid mass $m \approx 2 \times 10^{-25}$ Kg.

with the pedagogical example of the linear chain. That marks the onset of superposition of all exponential channels of all modes. In both cases, we find that the late stage of relaxation is to a good extent captured by a stretched exponential law. A more refined analysis can be

performed by calculating an effective decay exponent, defined as

$$\beta_e = \frac{d\left[\log[-\log \mathcal{D}(t)]\right]}{d\left[\log t\right]} \tag{41}$$

where

$$\mathcal{D}(t) = -\log\left[\frac{\langle E(t)\rangle - \langle E(\infty)\rangle}{\langle E(0)\rangle - \langle E(\infty)\rangle}\right] \quad . \tag{42}$$

Such measure is plotted in the insets of Figures 6 (a) and (b). One can appreciate that the decay follows for at least four decades a stretched exponential law whose exponent slightly oscillates with small frequency, corresponding to a relative variation in the range $10 \div 20$ %. It should be stressed that eventually the decay will speed up again to a pure exponential, on a time scale of the order $\mathcal{O}(N^3)$. This is the effect of having a finite system and hence one last mode that will eventually be left with all the residual energy of the system. However, the amount of energy left in the system at the onset of the last exponential stage shall be so small to make it by all means undetectable. On the contrary, from Fig. 6 it can be clearly ascertained that the first crossover occurs when the energy surplus left in the system is in the range of 20 % (Myoglobin) to 30 % (cluster) of the initial energy excitation, namely

$$\begin{aligned} \langle \Delta E(\tau_0)\rangle &\approx 0.2\,\langle E(0) - E(\infty)\rangle \quad \ldots \quad \text{Myoglobin} \\ \langle \Delta E(\tau_0)\rangle &\approx 0.3\,\langle E(0) - E(\infty)\rangle \quad \ldots \quad \text{Cluster} \quad . \end{aligned}$$

3 Relaxation in nonlinear systems

We have seen so far what happens in linear systems characterized by different spatial arrangements when they get coupled to a thermal bath through their surface. The picture that we have outlined appears to be rather general and to a large extent independent of the structural details. One can now ask how the whole picture would change if nonlinear potentials are introduced. The surprising answer to that question is *spontaneous localization of energy*. Quite generally, no matter the details of the nonlinearity included in the potential energy, it is found that edge cooling results in the emergence of long-lived localized vibrations in the lattice. Such vibrational modes are usually reminiscent of localized solutions of the corresponding Hamiltonian lattice, known under the general denomination of discrete breathers (DB) [43,44]. These are localized modes with an exponentially decaying envelope possessing one vibrational degree of freedom, whose characteristic frequency lies out of the linear spectrum of the system. One clear examples is the FPU lattice, where the residual state typically obtained upon edge cooling strongly resembles the *chaotic bretahers* obtained in the Hamiltonian system (no damping) upon modulational instability of band-edge waves [45].

As we shall outline in the rest of the paper, the properties of such self-localized excitations of sheer nonlinear origin may be very different from one system to another. However, it is a general fact that the extraction of energy from the surface allows a system to be directed to a region of its phase space dominated by quasi-periodic orbits, whose lifetime

is virtually infinite on the time scale accessible to numerical computation or otherwise free from random deviations due to round-off errors. We call this state a *pseudo-stationary state*. It is not a full non-equilibrium steady state because we are dealing with systems that are only subjected to damping, i.e. no external force capable of maintaining such dynamical equilibrium is taken into account. Hence, the observed pinning of energy will eventually disappear. However, it has been shown that the decay is exponential but with an *infinitesimal* decay constant [25]. This fact can be easily understood by noting that the decay rate of the pseudo-stationary state is controlled by the amplitude of vibrations of those particles lying at the surface. However, when energy is localized in the form of DBs, the amplitude decreases exponentially away from the centre of the mode, thus making the system overall virtually disconnected from the environment.

In the following, we shall analyze the main phenomenology of the process of self-localization by reviewing the results obtained in the case of the Fermi-Pasta-Ulam (FPU) potential and in the case of a linear chain of rotators. Moreover, I shall present a hint of recent results on spontaneous emergence of localized modes of nonlinear origin in a three-dimensional network of nonlinear oscillators. I will describe what is known so far, but more importantly this will lead me to clearly state what is still debated. Notably, two main points deserve to be anticipated at this stage.

1. What is the robustness of the process of spontaneous localization with respect to the introduction of a true thermal bath at the edges replacing the mere linear damping. That is, what would be the effect of external fluctuating forces on the localized modes. It seems that, at least in certain cases, a small amount of fluctuations chosen e.g. so as to satisfy a fluctuation-dissipation relation with the dissipative terms suffice to largely hinder the localization process. Besides being interesting *per se* in the first place, this analysis would in my opinion contribute to the understanding of what may be called a discrete breather at non-zero temperature. A question that remains largely open [46].

2. The second point still to be clarified concerns the exact nature of the attractor that characterizes the pseudo-stationary state of the damped systems. From one side, it is tempting in some cases to point out the strong similarity of the localized objects obtained in the long time limit with chaotic breathers [45] or other types of solutions pertaining to the undamped Hamiltonian systems. This is the case for example of DBs appearing in edge-damped FPU lattices as compared to the self-localized solutions emerging from the process of modulational instability in the Hamiltonian systems [31]. However, this resemblance, although convincing, is only qualitative. Quantitative studies on the comparison of these breathers with the chaotic ones obtained from modulational instability should be performed.

In the spirit of point 2, the results on self-localized excitations in optically trapped Bose-Einstein condensates from Ref. [24] are particularly remarkable. In fact, the authors compare the spontaneously emerging localized modes with available accurate analytical expressions describing localized vibrations in the Hamiltonian limit. They find no appreciable

difference within numerical uncertainty, thus suggesting that the system is indeed driven toward a *typical* attractor. This result, if confirmed in other systems, may have a profound significance. The process of edge cooling would be boosted to the role of an invaluable tool to profit of natural energy fluctuations to automatically select specific regions of the phase space. The experimental implications opened by this scenario would also be immense.

3.1 The FPU potential

In 1955, reporting about one of the first numerical experiments ever performed, Fermi, Pasta and Ulam remarked that it was " ... very hard to observe the rate of *thermalization* or mixing ... " in a nonlinear one-dimensional lattice in which the energy was initially fed into the lowest frequency mode [47]. Since then, the FPU potential has aroused much interest, not only with regard to the general problem of energy equipartition in nonlinear system, but also with regard to the new class of localized solutions named discrete breathers [13, 48]. The complete FPU potential is a nearest-neighbour potential of the form

$$V(u_{p+1}-u_p)=\frac{k}{2}(u_{p+1}-u_p)^2+\frac{\alpha}{3}(u_{p+1}-u_p)^3+\frac{\beta}{4}(u_{p+1}-u_p)^4 \qquad (43)$$

In the following, we will be only concerned with the quadratic plus quartic version ($\alpha=0$), also known as $\beta-$FPU.

Here we will focus on the study of the system response when energy is being extracted from its surface. More precisely, the general outline of the numerical experiments presented is the following. The lattice is prepared at an equilibrium condition, whereby all N particle displacements are zero and the velocities are drawn at random from a Maxwellian distribution with zero mean and standard deviation $\sigma=\sqrt{2E(0)/N}$. Then a short transient is performed by integrating the equation of motion with zero damping, which is meant to let the system equilibrate and reach a stable state of energy equipartition among the linear modes. It should be stressed that all simulations here are performed with a value of the initial energy density $E(0)/N$ above the strong stochasticity threshold, which marks the crossover to the regime where energy equipartition occurs on times scaling exponentially with the system size [49]. Successively, the dissipative dynamics is started and a one-way flow of energy is maintained through the surface, in the same way as we have seen for the harmonic chain.

It is useful to introduce the so–called symmetrized site energies e_p, which are given by

$$e_p(t)=\frac{1}{2}m\dot{u}_p^2+\frac{1}{2}\left[V(u_{p+1}-u_p)+V(u_p-u_{p-1})\right].$$

The istantaneous total energy of the system is then given by

$$E(t)=\sum_{p=0}^{N-1}e_p(t). \qquad (44)$$

Due to the presence of dissipation, the initial energy $E(0)$ will decrease in time. Since we are interested in determining the decay law of the quantity $E(t)/E(0)$, it is convenient to introduce the following indicator

$$\mathcal{D}(t) = \log[-\log(E(t)/E(0))]. \tag{45}$$

By plotting $\mathcal{D}(t)$ in semi-logarithmic scale, a streched–exponential law of the form $E(t)/E(0) = \exp[-(t/\tau)^\sigma]$ becomes a straight line with slope σ and y–axis intercept $-\sigma\log(\tau)$. This representation is particularly useful in identifying pure exponential regimes and crossovers to slower decay laws.

Most of all, we are interested in the effects of energy localization on the relaxation features. We then introduce a localization parameter $\mathcal{L}$, which provides a rough overall estimate of the degree of energy localization in the system. It is defined as

$$\mathcal{L}(t) = \frac{N}{E(t)^2}\sum_{p=1}^{N} e_p^2(t) \tag{46}$$

According to its definition, the fewer sites the energy is localized onto, the closer $\mathcal{L}$ is to N. On the other hand, the more evenly the energy is spread on all the particles, the closer $\mathcal{L}$ is to a constant of order 1. In particular, this indicator for the β–FPU potential studied here lies within the interval [7/4, 19/9], the two extremes being the energy–independent values of the harmonic and pure quartic potentials, respectively [45].

To minimize fluctuations, both the energy relaxation and the localization parameter curves presented in the following are the result of averaging over many realizations of the same initial condition, unless explicitly specified otherwise.

3.1.1 Relaxation in 1D

The equation of motion for the linear FPU chain with surface damping read

$$\begin{aligned} m\ddot{u}_p &= V'(u_{p+1}-u_p) - V'(u_p - u_{p-1}) \quad p = 2,3,\ldots,N-1 \\ m\ddot{u}_1 &= V'(u_2-u_1) - m\zeta\dot{u}_1 \\ m\ddot{u}_N &= -V'(u_N - u_{N-1}) - m\zeta\dot{u}_N \end{aligned} \tag{47}$$

with $V(x) = x^2/2 + \beta x^4/4$. With no loss of generality one can consider $\beta = 1$, since changing β simply amounts to an overall rescaling of the (initial) energy of the system. Moreover, we shall always express times in units of $\omega_0^{-1} = \sqrt{m/k}$. In particular, the damping strength will be specified by the usual non-dimensional parameter $\eta = \zeta/\omega_0$.

In Fig.7 the typical outcome of a relaxation experiment in a system with free-end boundary conditions is shown in the form of a space-time contour plot of the energy density field. Initially, the energy density is approximately a fraction of the same order at all sites. After a time of the order of $\tau_0 = N/2\eta = 500$, localized structures are seen to emerge at random sites, which eventually will coalesce into one single vibration localized onto a few sites with

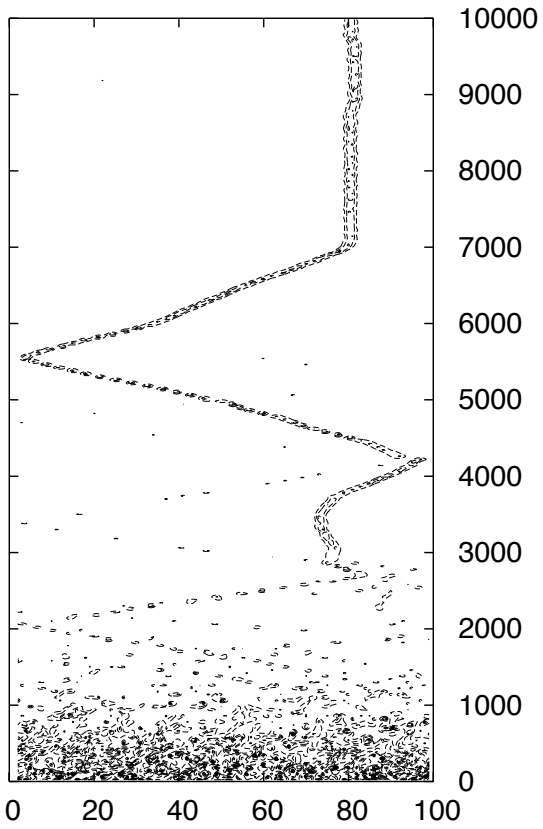

Figure 7: Space–time contour plot of the site energies. Time flows up and the horizontal axis is the site index. Parameters are $N = 100$, $\eta = 0.1$ and $E(0)/N = 1$. Reprinted with permission from Ref. [31]. Copyright 2005, American Institute of Physics.

an energy higher than $E(0)/N$. In the long run, the localized mode that has self-localized is seen to wander around with approximately constant velocity, rebound onto the cold surface and eventually get stuck again at some position in the chain. After that it will probably start displacing again, possibly alternating states of stillness and movement. The velocity of displacement is strongly sub-sonic (it can be estimated to be about $0.1 \ll c = 1$ from the figure in this particular case), as it seems to be typical of moving nonlinear excitations in nonlinear lattices. In fact, in the low energy limit it can be shown that travelling discrete breathers tend to the small amplitude envelope solitons solutions of the Korteweg-de Vries equation [50].

Fig. 8 reports an analysis of the relaxation along the single trajectory shown in Fig. 7. In panel (a) the rise of the localization parameter signals that energy is being focused onto fewer and fewer sites as times goes by. It is interesting to observe that in general a function

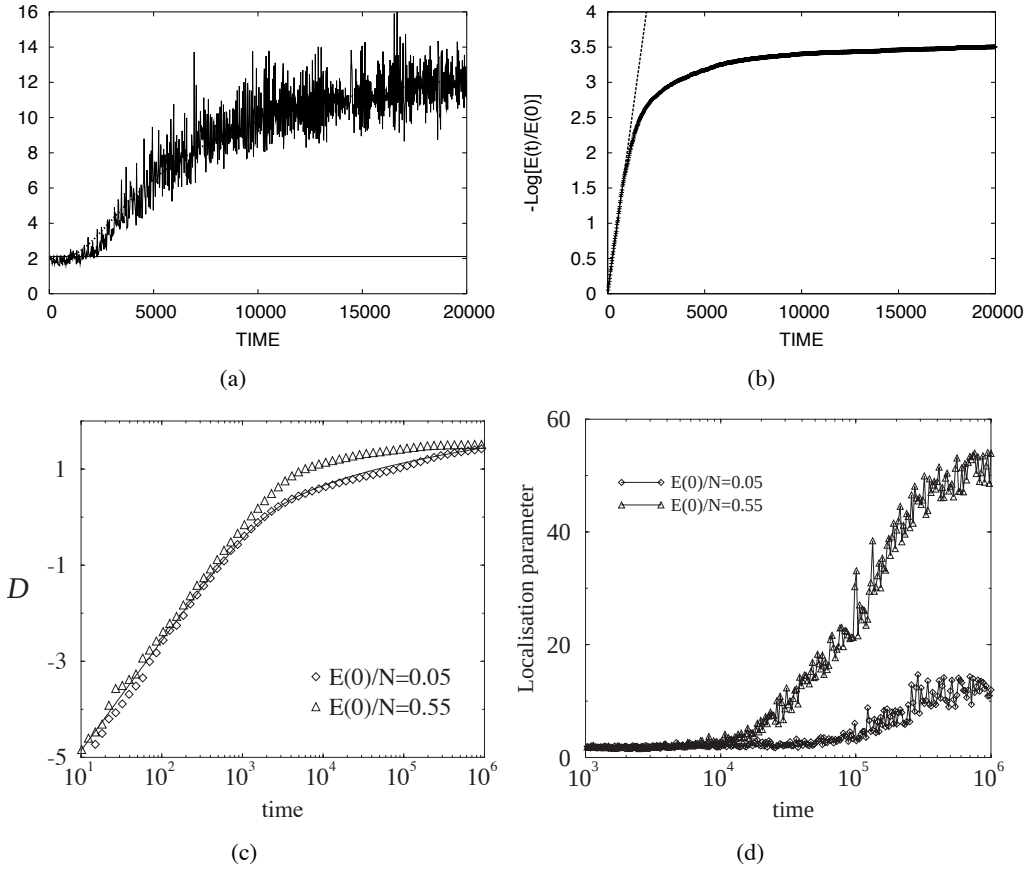

Figure 8: (a) Localization parameter calculated for the trajectory shown in Fig. 7. The horizontal line marks the asymptotic value $\mathcal{L}_h = 19/9$ of the harmonic chain. The thick line is a fit with the function (48), which gives an asymptotic value $\mathcal{L}_\infty = 15.5$ and a localization time $t_0 = 5576.5$. (b) Total energy decay curve for the same trajectory. The solid line is a plot of the exponential law $E(t)/E(0) = \exp(-t/\tau_0)$. Parameters are $N = 100$, $\eta = 0.1$ and $E(0)/N = 1$. (c) Semilogarithmic plot of the indicator DLE (Eq. 45) averaged over 32 realizations of the same initial conditions for an FPU chain with free ends. The solid line is a plot of the expected behaviour in the linearized system: $E(t)/E(0) = \exp(-t/\tau_0)\, I_0(t/\tau_0)$. (d) Corresponding averaged localization curves. Parameters are: $N = 256, \eta = 0.05$. Figures (c) and (d) are reproduced from Ref. [25] with permission from IOP publishing.

of the type

$$\mathcal{L}(t) = (\mathcal{L}_\infty - \mathcal{L}_h)e^{-t_0/t} + \mathcal{L}_h \tag{48}$$

provides a good fitting of the numerics. Here $\mathcal{L}_\infty$ is the asymptotic value of the localization parameter corresponding to the fully formed breather in the pseudo-stationary state, while $\mathcal{L}_h = 19/9$ is the average value that characterize an harmonic chain with the same parameters. Such choice of the fitting function suggests that overall the process by which

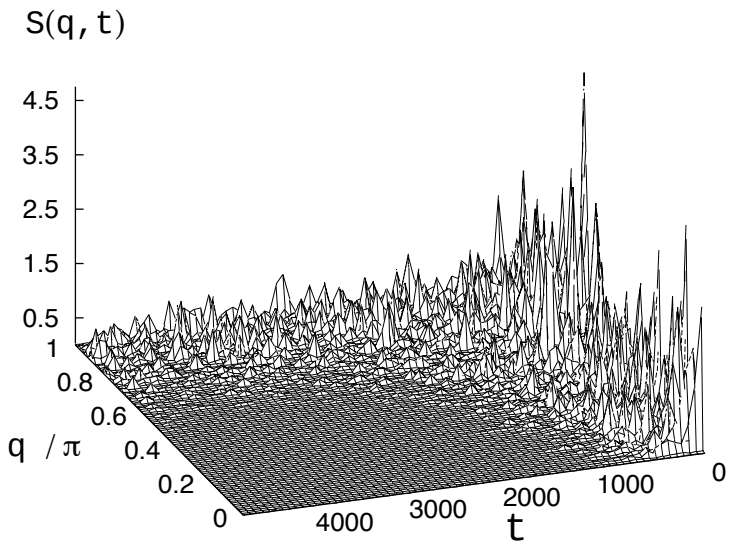

Figure 9: Surface plot of the time–dependent spatial spectrum of particle velocities for a one-dimensional FPU lattice with free ends. Parameters are $N = 100$, $\eta = 0.1$ and $E(0)/N = 1$. Reprinted with permission from Ref. [31]. Copyright 2005, American Institute of Physics.

the breather gathers its energy along its localization pathway implies some *diffusion* of energy along the chain. Panel (b) reports the decay curve of the system energy. It can be clearly appreciated that the first relaxation stage proceeds exponentially with decay time $\tau_0 = N/2\eta = 500$. Recalling the analysis performed in the harmonic chain, we thus conclude that it is the linear mode that is characterized by the highest decay rate that controls this first stage. That is, being the ends free, energy is being rapidly extracted from the lowest-frequency mode. At a characteristic time τ_0 a crossover occurs and the energy decay slows down. In the long run, a pseudo-stationary state is attained, corresponding to the onset of spontaneous energy coalescence into a single discrete breather. At this stage, the system energy saturates to an asymptotic value corresponding to about 3 % of the initial energy. This means that an energy about three times greater than the initial specific energy $E(0)/N = 1$ ended up being stored into the breather in this particular realization. We conclude that the phenomenon of spontaneous localization did not affect the transient decay appreciably. It is worthwhile to stress that the time scale for the crossover observed in the total energy relaxation and the characteristic time for localization are widely separated time scales (see caption of Fig. 8 (a)). We have thus learnt that in the case of a FPU chain it is extremely misleading to infer a signature of the process of spontaneous localization from the energy curve.

The above conclusion can be made even more evident by repeating the same experiment for lower values of the initial energy density and taking averages over different initial conditions. Fig. 8 (c) shows very clearly that the discrepancies in the transient regime

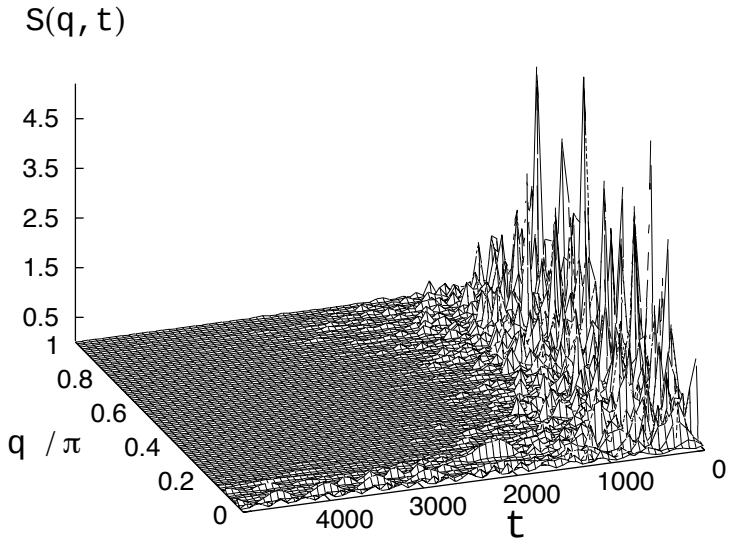

Figure 10: Surface plot of the time–dependent spatial spectrum of particle velocities for a one-dimensional FPU lattice with fixed ends. Parameters are $N = 100$, $\eta = 0.1$ and $E(0)/N = 1$. Reprinted with permission from Ref. [31]. Copyright 2005, American Institute of Physics.

of the relaxation between the FPU system and its linearized counterpart are virtually suppressed for sufficiently small values of the initial specific energy. As a matter of fact, for $E(0)/N = 0.05$ the theoretical prediction (10) perfectly interpolates the average decay of energy before the FPU chain reaches its asymptotic state. Nonetheless, the system is showing something profoundly new, a localization process of sheer nonlinear origin is taking place, as it is manifest from the localization curves plotted in Fig. 8 (d).

All the above considerations suggest that the process of spontaneous formation of DBs follows a path which can be still described in terms of the multi-channel relaxation of linear modes. This can be simply verified by looking at the time-dependent spatial spectra of the velocity field in the course of the relaxation process. Fig. 9 shows that indeed the free-end relaxation spectrum of the harmonic chain (Eq. 7) rules the overall decay during the transient. Consequently, low-frequency modes soon disappear from the picture, leaving all the residual energy in the band-edge modes The above picture is strongly reminiscent of the process of creation of *chaotic breathers* in Hamiltonian FPU chains where energy is initially stored in the $\pi-$mode with a little long-wavelength modulation [45]. In that case, the $\pi-$mode is modulationally unstable, and through a pathway similar to that shown here in Fig 7, all energy ends up focused in a localized mode wandering without appreciable energy loss through the lattice. It is thus tempting to draw a direct analogy between the two scenarios and advocate a role for modulational instability in the present context.

An argument in favour of such interpretation comes from the study of the FPU chain with fixed ends. In this case, the above considerations lead to speculate that the long-

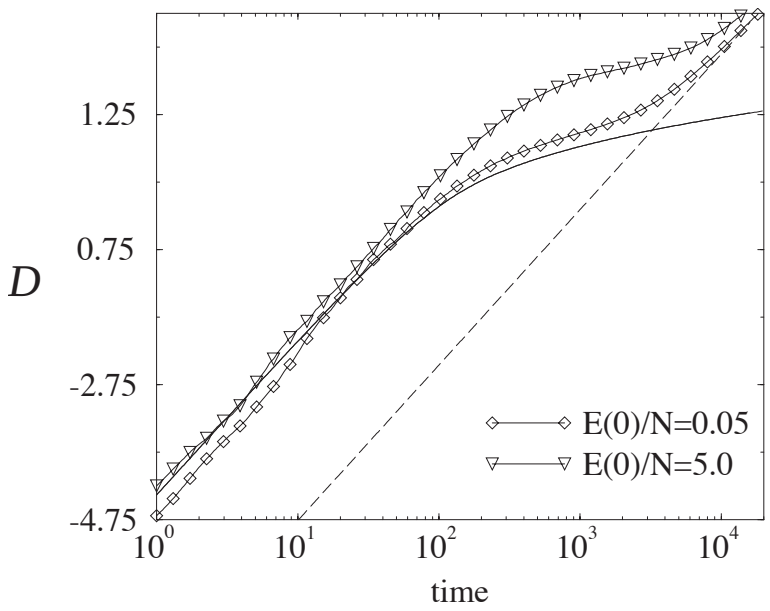

Figure 11: Solid lines with symbols: plot of $\mathcal{D}(t)$ for an FPU chain with fixed ends for $E(t)/E(0)$ =0.05 and 5. The solid line is a plot of the theoretical prediction (10). The dashed line is the exponential law $\exp(-2t/\tau_{N-1})$, with $\tau_{N-1} = N(N+1)^2/2\pi^2\eta$. The numerical data are the result of averaging over 32 initial conditions. Parameters are $N = 16$, $\eta = 0.05$.

wavelength modes will display much longer lifetimes, according to the spectra (7). More importantly, the band-edge modes should be suppressed faster with respect to the case of free ends (see again Fig. 2 (b)). In this case, a process of modulational instability is expected to be strongly hindered because of the fast disappearance of band-edge modes, not to mention the protracted coexistence of long- and short-wavelength vibrations. Fig. 10 shows that in a typical simulation the time evolution of the mode energies indeed again follows the prescriptions of the linearized relaxation spectrum. After some time, the band-edge modes have disappeared completely from the picture, and the little residual energy is stored in long-wavelength vibrations: modulational instability might not have even had the time to set the localization process in motion, since the unstable modes have been rapidily swept away. Indeed, spontaneous localization is hardly ever observed in the fixed-ends system. Fig. 11 shows that the total energy decay follows in this case the theoretical prediction of the linear chain at all times. In particular, after a crossover to an inverse-power law, the energy typically ends up decaying exponentially again with half the lifetime of the longest-wavelength mode. No difference at all with an harmonic chain, but for a slight dependence on the initial energy of the time characteristic of the first crossover. Somewhat paradoxically, the more energy is stored in the chain in the beginning, the longer seems to be the first exponential stage, extending past τ_0.

3.1.2 Relaxation in 2D

We have seen that the onset of spontaneous localization in a FPU chain is is related in a subtle fashion to the characteristic of the total energy decay. In particular, in spite of the nonlinearities, whenever localization does not occur, it is difficult to discern the nature of the system from the energy relaxation. This is the case, for example, of the FPU chain with fixed ends. There is another case where this effect also occurs, namely in FPU systems of dimension greater than one.

It is known that, depending on the details of the non-linear potentials, the energy vs frequency relation for a breather solution in more than one dimension may show a non-vanishing breather energy as the frequency approaches the edge of the linear band from above. In particular, breather energies have a positive lower bound if the lattice dimension is greater than or equal to a certain critical value d_c that can generically be equal or greater than two for a large class of Hamiltonian systems. In the case of the FPU potential $d_c = 2$ [51, 52]. As a consequence, we expect that the emergence of spontaneous localization in a two-dimensional FPU lattice will show the features of a *thermally activated* process. This means that if not enough energy is stored initially in the lattice in order for a sufficiently large fluctuation to occur, no breather might be excited and the energy decay will follow the law of harmonic lattices in 2D.

I consider here a scalar model of an $L \times L$ square lattice of identical particles of mass m with $\beta-$FPU coupling between nearest neighbours with one degree of freedom $u_{i,j}$ per lattice site. The equations of motion read

$$\begin{aligned} m\ddot{u}_{i,j} = & V'(u_{i+1,j} - u_{i,j}) - V'(u_{i,j} - u_{i-1,j}) + \\ & V'(u_{i,j+1} - u_{i,j}) - V'(u_{i,j} - u_{i,j-1}) - m \sum_{p,q=0}^{N-1} \Gamma_{ij}^{pq} \dot{u}_{p,q}, \end{aligned}$$

where $V(x)$ is the FPU potential (43) with $\alpha = 0$ and Γ is the damping matrix specifying coupling with the environment on all four sides of the lattice

$$\Gamma_{ij}^{pq} = \zeta \left[g_{ip}\delta_{j,q} + \delta_{i,p} g_{jq} - g_{ip} g_{jq} \right]$$

with $g_{ip} = \delta_{i,p}[\delta_{p,0} + \delta_{p,N-1}]$, δ_{ij} being the usual Kronecker symbol. Boundary conditions are taken to be of the free-ends type.

Calculations identical to those reported in section 2.1 can be easily extended to obtain the energy decay curves corresponding to the linearization of Eqs. (49). It turns out that the contributions from the two spatial coordinates are identical for an $L \times L$ lattice, and therefore factorize, yielding

$$\frac{E(t)}{E(0)} = \left[e^{-t/\tau_0} I_0 \left(\frac{t}{\tau_0} \right) \right]^2 \approx \begin{cases} e^{-2t/\tau_0} & \text{for } t \ll \tau_0 \\ \dfrac{1}{2\pi(t/\tau_0)} & \text{for } t \gg \tau_0 \end{cases}, \tag{49}$$

with $\tau_0 = L/2\eta$.

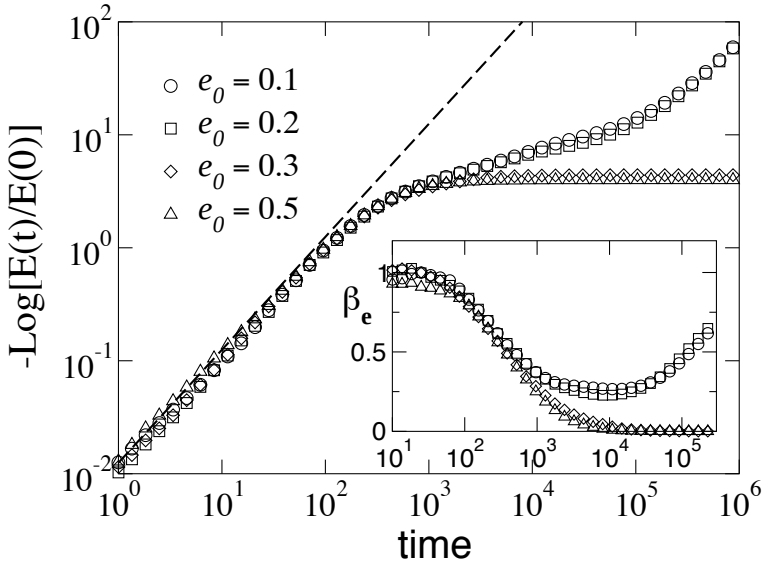

Figure 12: Energy decay curves for a square FPU lattice of side L for different values of the initial energy density. The dashed line is plot of the exponential law $\exp(-2t/\tau_0)$. The inset shows the corresponding effective relaxation exponents calculated from Eq. (41). Parameters are $N = L^2 = 32 \times 32$, $\eta = 0.1$. Reprinted with permission from Ref. [26]. Copyright 2003, American Institute of Physics.

In Fig. 12 I report the energy decay curves obtained by numerically integrating Eqs. (49) with equilibrium initial conditions corresponding to different values of the initial energy density $e_0 = E(0)/N$. As a first observation, we see that the first stage of the relaxation is again captured by the exponential law specified by the analysis of the linearized system. A crossover also exists on the time scale τ_0. However, at variance with the 1D case, the fate of the dynamical evolution after the crossover depends here on the initial energy density. It is immediately evident that a specific energy at least above $E(0)/N = 0.2$ is required in order to trigger spontaneous localization. Otherwise, the decay does not saturate and accelerates again to the finite-size exponential. This is made evident also by the plots of the effective exponent β_e shown in the inset of Fig. 12. This is a clear manifestation of the existence of an *energy threshold* for the creation of a breather.

Threshold excepted, the relaxation process described in terms of the energy decay curves is identical to the picture which applies to the 1D FPU case. Nonetheless, the scenario markedly differs from the 1D case in another fundamental respect: the mobility of the localised excitations that spontaneously emerge appears drastically reduced. In fact, after a first stage in which strong interaction is observed, breathers generally arrange on a "random lattice", which, on the time scale of a typical simulation, appears indeed to be frozen. One of such states is illustrated in Fig. 13. This is presumably due to a smaller "scattering section" in 2D and may also reflect a degree of *frustration* in the breather mobility. Note that the average energy stored into one breathers is of the order of 10 or more, i.e. ten times at

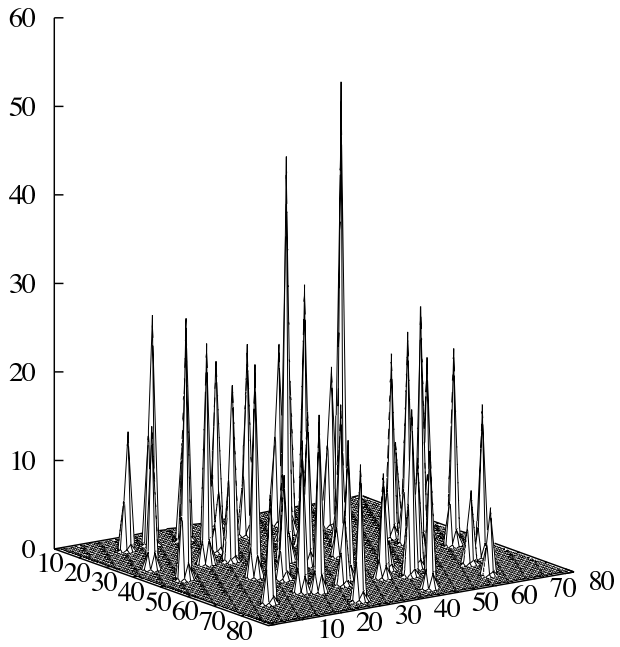

Figure 13: Surface plot of the symmetryzed site energies in the residual state in a 2D FPU square lattice. Parameters are: $L = 80$, $\eta = 0.1$, $E(0)/N = 1$. Reprinted with permission from Ref. [26]. Copyright 2003, American Institute of Physics.

least greater than the initial energy per particle, with cases where a single breather captured up to 50 times the initial energy density.

The energy threshold As a consequence of the existence of an energy threshold Δ for creating a breather, we expect that localised modes are generated in the relaxation dynamics only by fluctuations that are large enough to overcome such threshold. The spontaneous excitation of breathers can thus be seen as an activated process. Accordingly, their number will be exponentially small in the ratio between Δ and some quantity measuring the strength of fluctuations. Therefore, one expects the average density of breathers (i.e. the average number of breathers per lattice site) in the residual state to follow an Arrhenius law of the form

$$\langle n_B \rangle \propto e^{-\beta\Delta} \quad . \tag{50}$$

From Eq. (50), it is tempting to identify β with the inverse temperature. However, one has to keep in mind that we are dealing with a non–equilibrium process and this identification can only make sense if the energy release is adiabatically slow. If this is true, $1/\beta$ should be proportional to (and smaller than) the initial temperature, which, in turn, is proportional to the initial energy density by construction of our simulation scheme.

The numerical simulations clearly confirm that n_B strongly depends on the initial spe-

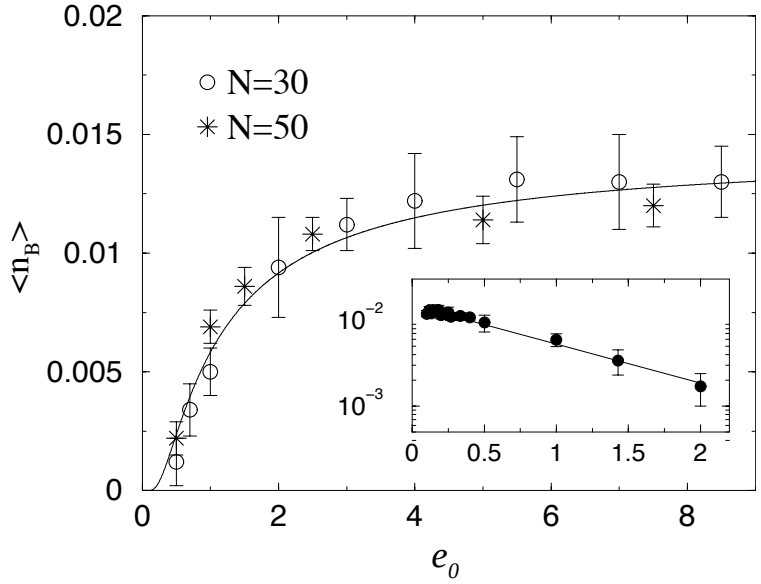

Figure 14: Average breather density $\langle n_B \rangle$ vs initial energy density for $L = 30$ and $L = 50$ and Arrhenius plot. The inset shows the average density measured in the system with $L = 50$ vs $1/e_0$ in lin–log scale, and an exponential fit. Reprinted with permission from Ref. [26]. Copyright 2003, American Institute of Physics.

cific energy. In Fig. 14 I plot $\langle n_B \rangle$ as calculated from a large ensemble of events for two values of the system size as a function of e_0, along with a fit performed with the law $\langle n_B \rangle = C \exp(-\Delta'/e_0)$, with $\Delta' \propto \Delta$. As it shows, the agreement is good. Hence, the spontaneous localisation of energy triggered by edge cooling is indeed an activated process. In particular, the fit gives $\Delta' \approx 0.9$. We note that a quantitative analysis of the time t_0 required to reach the residual state (localisation time) reveals that $t_0 \propto 1/\langle n_B \rangle \propto \exp(\beta\Delta)$. By fitting the numerical data for the localisation time, it is possible to get an independent confirmation of the thermal activation scenario. In particular, this calculation gives $\Delta' \approx 0.7$, in good agreement with the value obtained above [53]. In Ref. [26] it is also shown that the values of the parameter β extracted from the numerics indeed satisfy an inverse-proportionality relation with the initial energy density $1/\beta \propto E(0)/N$, which proves that localization is a true thermally activated phenomenon in this case.

3.1.3 The lesson of FPU

The original claim of Aubry and Tsironis in 1996 was that the energy decay of an edge-damped system bears the clear signature of spontaneous emergence of localized excitations. More precisely, they claimed that the energy slowed down to a stretched exponential [11] in contrast to the *usual* exponential relaxation characteristic of harmonic systems. After the work of Piazza, Lepri an Livi in 2001 [25], we now know that the latter inference is not

necessarily true, and much care is to be taken when looking at the energy decay. In fact, we have just learnt that the relaxation not always shows the fingerprint of energy localization. FPU systems are paradigmatic examples of such subtleties.

What emerged clear from subsequent studies, is that the average energy decay curves should be always thought of as consisting of two stages. I shall call the first stage the *transient* and the second one the asymptotic stage. The first seems to typically cross over to the second on a time scale of the order of τ_0. For example, in FPU systems the transient is an exponential with the same time constant. The asymptotic stage characterizes the post crossover stage. If energy is localized, the latter coincides with the pseudo-stationary state, where energy still flows out of the system but with an exponentially small time constant that makes any decay *de facto* undetectable no matter how long one integrates the equation of motion. If otherwise energy does not localize, the system shows little deviations from the behaviour of its linearized version. Which, in turn, is far from trivial.

However, the picture got more complicated with the help of subsequent pieces of investigation. It emerged that the transient also should in general be thought of consisting of two sub-stages. The first one is the familiar exponential $\exp(-t/\tau_0)$, but an itermediate slow down before the energy is ultimately pinned can occur. Following intuition, this is the case for example if an on-site anharmonic potential is added to an FPU chain [26]. In that case, for small values of the ratio between local and inter-particle couplings, the picture does not deviate from what we have just seen for the FPU chain. However, by reversing that ratio, an intermediate crossover is observed to a stretched exponential law that sets in before the eventual creation of a localized structure and and energy pinning. This effect is reported here in Fig. 15 in the case where the on-site potential is a quartic function of the type $U(u_p) = \kappa u_p^4/4$ with variable strength κ. Note that the characteristic time of departure from the initial exponential is much smaller than τ_0, which still approximately marks the onset of the pseudo-stationary state. In this case, the transient energy decay bears the distinctive signature of the energy localization process.

It is clear that energy is being localized in both cases (see panel (b) of the same figure). The question is then: what features of the localization pathway cause the system to slow down onto a stretched exponential? One may think at that point that the presence of a strong *dynamical discreteness* is to be associated with the emergence of a stretched exponential law (or equivalently another sub-exponential law) during the transient. In the following section I will provide an example that this is not the case. Rather, the emergence of a slower-than-exponential transient in the *average* behaviour of the system seems to bear a firmer relation with the nature of *single realizations*. In fact, what I have neglected to say is that not only a crossover to a stretched exponential law occurred in the average energy relaxation in the simulations reported in Fig 15. Another intriguing effect had made its apparition. Namely, the decay of energy during a single trajectory has now the shape of a step-wise process, whereby the energy preferentially flows out in bursts, causing energy jumps followed by plateaus where energy hardly drains away.

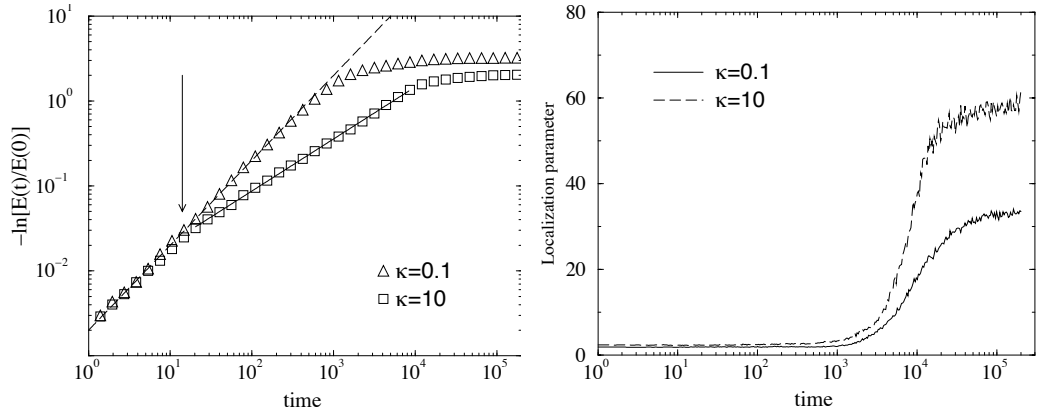

(a) (b)

Figure 15: FPU chain with quartic on–site potential. (a) Plot of $\mathcal{D}$ vs time. The dashed line is the exponential $\exp(-t/\tau_0)$, while the solid line is a fit with the stretched exponential law $\exp[-(t/\tau)^\sigma]$ ($\sigma \approx 0.6$). The arrow marks the time at which the system with $\kappa = 10$ departs from the initial exponential trend. (b) Localisation parameter vs time for different values of the on–site coupling κ. The data of both $\mathcal{D}$ and $\mathcal{L}$ are averaged over 32 initial conditions. Parameters are $N = 100$, $\eta = 0.1$ and $e_0 = 1$. Reprinted with permission from Ref. [26]. Copyright 2003, American Institute of Physics.

3.2 The chain of rotators

In this section I shall review the results of edge relaxation experiments in a chain of rotators, with and without onsite potential. The main observations have been reported in a qualitative fashion in ref. [54], while a more accurate and systematic work has been published in ref. [27]. Anticipating the main point, we shall discover that the presence of a local term in the potential energy does not make any difference and the average relaxation of energy is always observed to follow a stretched exponential transient, prior to be nailed down in the quasi-stationary state. What is very clear from these simulations, is the step-wise character of the single realizations of the relaxation process, which are the true fingerprint of the appearance of a stretched exponential in the average behaviour.

We shall study the relaxation toward equilibrium of a chain of classical rotators coupled on a lattice with damping acting at its edges. The equations of motion are

$$I_i\ddot{\phi}_i = -G\sin\phi_i + K\left[\sin(\phi_{i+1}-\phi_i)+\sin(\phi_{i-1}-\phi_i)\right] - \nu\dot{\phi}_i\left[\delta_{i,1}+\delta_{i,N}\right] \qquad (51)$$

where ϕ_i in the angle variable of the i-th rotator (with $i = 1, 2, \ldots N$). The Hamiltonian version of (51) is sometimes referred to as the sine–lattice equations [55, 56]. Furthemore, we impose free–end boundary conditions ($\phi_1 = \phi_0$, $\phi_N = \phi_{N+1}$). In the following we shall be concerned with both the cases $G = 0$ and $G = 1$.

The difference between the behaviour of a single trajectory and the averaged relaxation is made very clear in Fig. 16. The step-wise character of a single realization is manifest: the

energy extraction proceeds by sudden lumps of energy being released through the boundaries, followed by stages where practically no energy is let out of the system. A deeper understanding of what is going on can be acquired by looking at space-time contour plots of the local energy field for some of these quasi-piecewise linear processes. The energy density contour plots show that the process is associated with the spontaneous creation of long–lived localized objects, characterized by a fast librating motion of a single rotator almost decoupled from its neighbors. These localized excitations (rotobreathers) have already been shown to exist in the Hamiltonian lattice [55]. The two outermost rotobreathers systematically act as barriers between a central "hot" region of the chain and its boundaries, thus blocking the energy flow toward the environment. At some stage, such dynamical barriers are spontaneously destabilized, thus allowing a portion of the trapped energy to be rapidly dispersed away. This process goes on progressively emptying the energy content of the central hot core until a single rotobreather survives in the bulk.

The conclusion is that the average of many step-wise processes results in a sub-exponential relaxation, well approximated by a stretched exponential law. Since different initial conditions are observed to give rise to substantially different sequences of jumps and plateaus, those may be regarded as different realizations of a stochastic process. Hence, we conclude that the peculiar nature of the *integrated* relaxation is related to the statistical properties of such stochastic process. Indeed, the accurate analysis performed in ref. [27] has shown that the stochastic process underlying the generation of sequences of energy jumps and time plateaus is stationary. For example, the average value of the plateaus does not vary by progressing into the series of relaxation stages. Rather, the distribution of time stretches between adjacent energy jumps can be well approximated with a stretched exponential law.

It is then not that a combination of simple statistics on the energy and time axes yields in this case a stretched exponential integrated regime. In ref. [27], the authors show how results from the theory of rare events may be used to cast the problem in other terms. Namely, they show that the energy flux autocorrelation function reveals long-range temporal correlations. This observation should be compared with what happens in FPU lattices, where a stretched exponential transient is not observed in parallel with an exponentially decaying autocorrelation of the energy flux. Since the transient dynamics is connected to the system's response, the obvious association that opens up is then with the transport properties of the system, notably heat conduction [57]. In this respect it should be recalled that the very same objects that spontaneously emerge during the transient have been invoked to explain the normal conduction in the model with $G = 0$ [58]. In this sense, the results here reviewed confirm the essential role of nonlinear excitations in the out–of–equilibrium properties of many–body systems.

Incidentally, the emergence of stretched exponential relaxation on average as a result of the superposition of many similar stepwise decay processes has been found also in two–dimensional easy–plane ferromagnets [59]. In such case, annihilation of vortex–antivortex pairs is the basic physical mechanism.

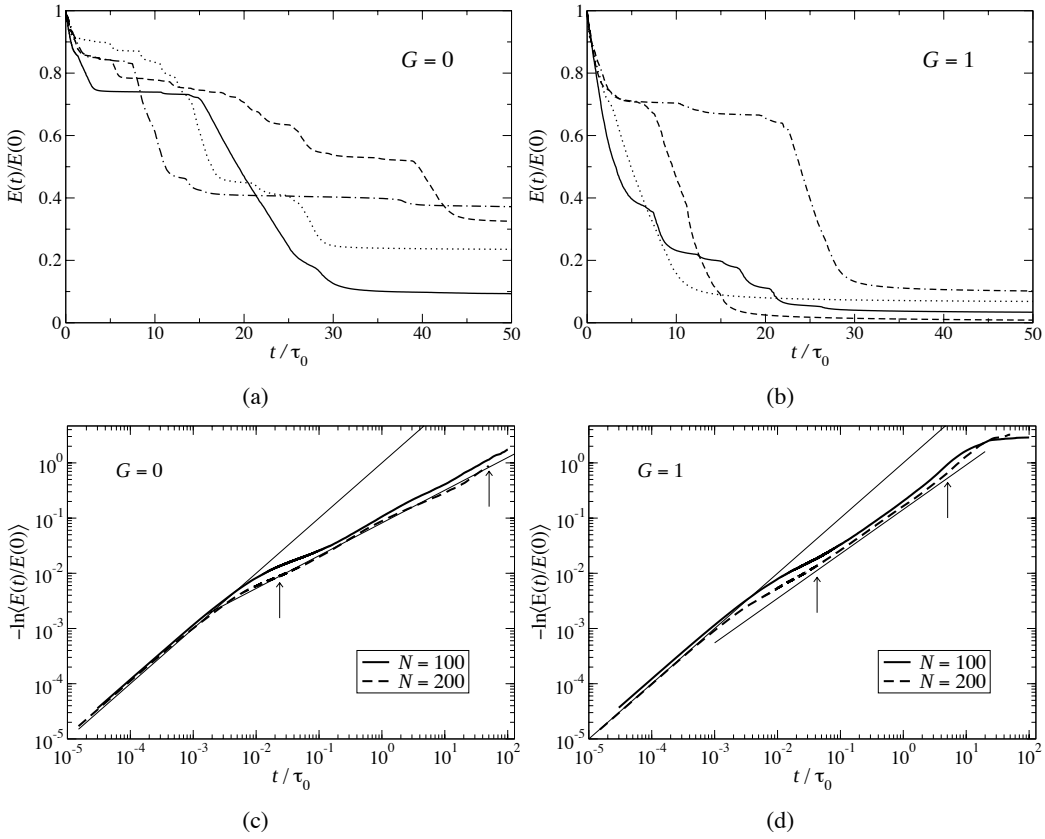

Figure 16: Upper panels: decay of the normalized total energy for four different initial conditions with $E(0)/N = 5$. (a) $G = 0$. (b) $G = 1$. Lower panels: decay of the normalized total energy averaged over a set of 99 initial conditions. (c) $G = 0$, (d) $G = 1$ We plot $-\ln\langle E(t)/E(0)\rangle$ in log–log scale with $E(0)/N = 5$ and for two different lengths of the chain. The thin lines correspond to $\exp[-t/\tau_0]$ (leftmost curve), and to a stretched exponential fit $\exp[-(t/\tau)^{\sigma}]$ of the data between the two arrows, with $\sigma = 0.80$ (c) and $\sigma = 0.59$ (d). Parameters are $N = 200$, $\nu = 0.1$, $K = 1.4911$. Reprinted from Ref. [27], Copyright (2005), with permission from Elsevier.

3.3 Nonlinear dynamics in proteins

Problems concerning localization and storage of energy by biomolecules are arousing increasing interest in the community at the interface between physics and biology [60, 61]. An intriguing example is enzymatic catalysis. How does an enzyme store and utilize the energy released at substrate binding? It is known that this energy may be deployed on much longer time scales (microsecond to millisecond) than those characteristic of the energetic process and at very distant places with respect to the catalytic site of the enzime [62]. While the chemical events and static structural features of enzyme catalysis have been extensively studied, very little is known about dynamic processes of the enzyme during the catalytic cycle. From Dynamic NMR methods such as ZZ-exchange, line-shape analysis,

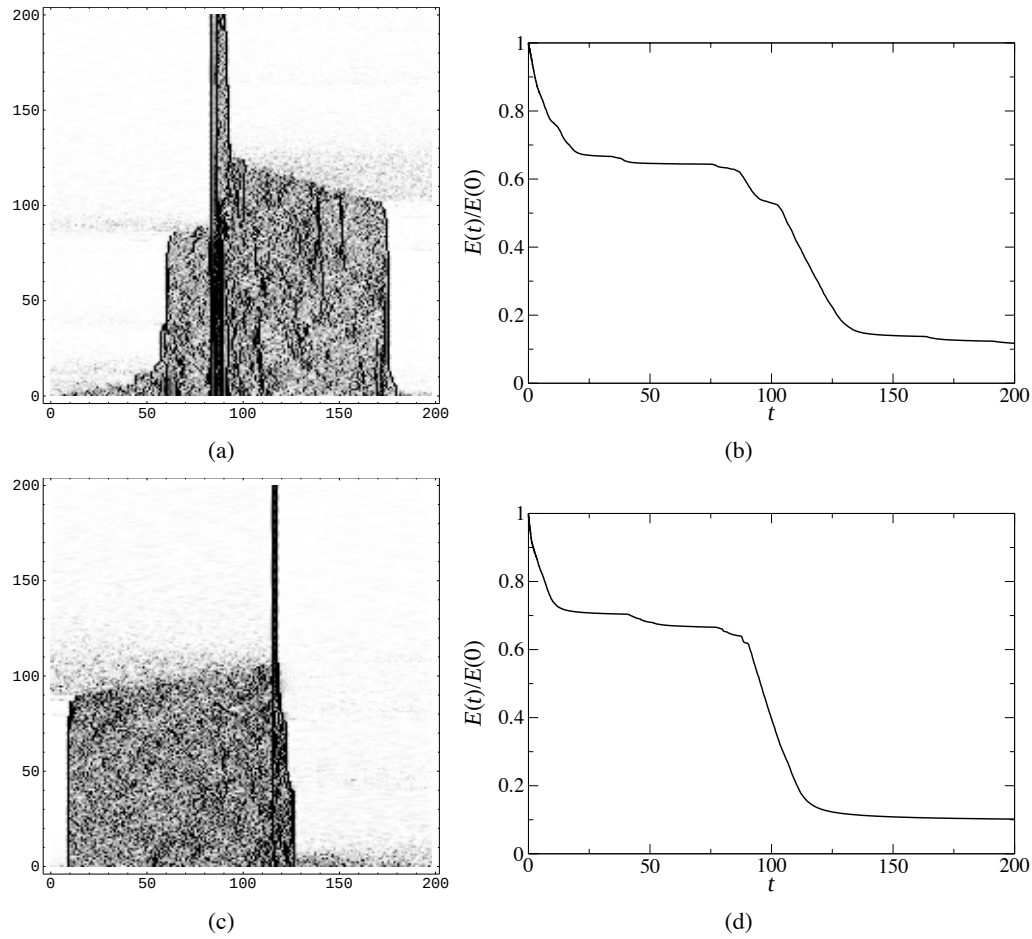

Figure 17: Relaxation in a chain with $N = 200, \nu = 0.1, K = 1.4911, E(0)/N = 5$. Upper panels $G = 0$, lower panels $G = 1$. (a), (c) Space–time density plots of the symmetrized site energies. The regions with higher energies are labeled with darker shades of grey. The chain sites i are reported on the horizontal axis ($2 \leq i \leq N - 1$), the vertical axis describes the time evolution in units of sampling times (250 natural time units). (b), (d) Decay of the normalized lattice energies. The time is expressed in units of the sampling time of the lattice site energies. Reprinted from Ref. [27], Copyright (2005), with permission from Elsevier.

Carr-Purcell-Meiboom-Gill (CPMG), and rotating frame spin-lattice relaxation a picture seems to arise in which flexibility in the microsecond to millisecond time regime is intrinsic and likely to be an essential feature of the enzyme [63]. Quantitative analysis of dynamics at multiple sites of the enzyme reveal large-scale collective motions, thus suggesting that low-frequency normal modes may embody the functional spatial correlation patterns [38]. In fact, the exchange of energy among collective modes in proteins have been investigated, unveiling that coupling between modes strongly depend on their geometrical overlap [64].

On the other hand, collective modes are also considered to be highly damped [65] and

alternative hypotheses have been formulated as to the ability of enzymes to efficiently store and transfer energy across their structures. Exploiting the existence of a high degree of non-linearity in protein dynamics, the excitations of localized vibrations in $\alpha-$helices similar to discrete breather has been proposed as the explanation of energy storage in enzyme catalysis [60, 66]. Other interpretations have also been formulated in the framework of the Davydov's soliton concept [67]. In this framework, energy transfer across helices would occur predominantly by hopping of localized vibrations along the chain resulting from non-linear coupling of spatially overlapping localized modes in resonance [68]. In fact, much work along these lines has been prompted by intriguing experimental results, whereby numerous subtleties in protein dynamics have emerged experimentally, notably through infra-red spectroscopy [69, 70]. Particularly interesting appear the results of Xie et al. [71], that reveal the existence of very long-lived oscillations in proteins rich in $\alpha-$ helices (such as myoglobin, bacteriorhodopsin) but not in proteins with a predominant $\beta-$sheet character (photoactive yellow protein) when excited by a far IR laser pulse.

3.3.1 Spontaneous localization upon surface cooling in Citrate Synthase

Up to this point, we have examined the phenomenon of spontaneous emergence of localized excitations in regular lattices coupled to the environment through their surface. In more than one dimension, we have seen that such phenomenon becomes *thermally activated* because localized modes cannot be excited below a characteristic energy threshold. Importantly, we have seen that the resulting pseudo-stationary state consists of a collection of tightly packed breathers that appear to form a sort of random lattice of localized modes. Since these modes appear through a phenomenon akin to modulational instability of band-edge modes, such peculiar spatial arrangement may be thought of expressing the extended character of the spatial pattern of those modes. In other words, since local fluctuations characterized by high frequencies are equally likely to emerge everywhere, a non-linear excitations developing from such events may localize at any point in the lattice with the same probability. This is in fact what is observed. One may ask what would be observed if the highest frequency modes were localized due to spatial disorder. In this case, the spatial pattern of those modes should make more likely a localized vibration to emerge at those sites where the spatial patterns of band-edge modes are localized. We shall see that this is in fact the case in protein structures, where the highest modes are indeed strongly localized at locations characterized by the highest local connectivities, i.e. regions of the three-dimensional structures where the local particle density is highest [72].

Anharmonic network model of Citrate Synthase Citrate Synthase is a two-domain enzyme that catalyzes the production of citrate upon binding to coenzyme A. Its three-dimensional structure is shown in Fig. 18 as determined from X-ray crystallography at 2.3 Å resolution. Here, we wish to extend the elastic network model introduced in section 2.3 in order to incorporate nonlinear effects. A natural choice is to build a three-dimensional network coarse grained at the amino acid level with the introduction of a specified cutoff for

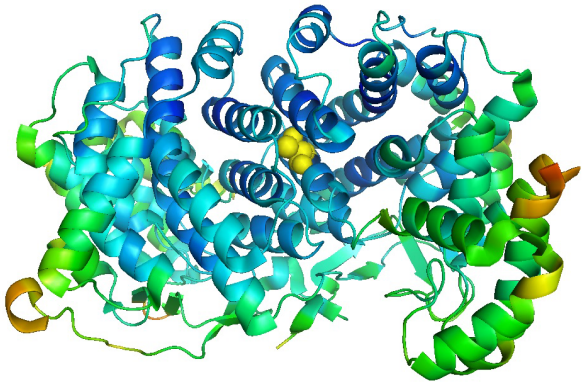

Figure 18: The three-dimensional structure of CITRATE SYNTHASE color-coded according to the measured atomic RMSDs, depicting the less mobile (blue) and the more flexible regions (PDBid: `1IXE`). The yellow spheres represent the residue Threonine 206.

pair interactions, and introduce nonlinear springs of the $\beta-$FPU type between interacting residues. Hence, we write the total potential energy of the protein as a sum of symmetryzed site energies

$$U(\{\vec{r}_i\}) = \sum_i e_i \tag{52}$$

where the site energies e_i are given by

$$e_i = \frac{1}{2}\sum_{j=1}^{N} K_{ij}\left[(|\vec{r}_i - \vec{r}_j| - |\vec{r}_{i0} - \vec{r}_{j0}|)^2 + \frac{1}{2}(|\vec{r}_i - \vec{r}_j| - |\vec{r}_{i0} - \vec{r}_{j0}|)^4\right] \tag{53}$$

Here K_{ij} is the contact map of the protein, which specifies the group of interacting neighbours for each residue by cutting off all particles lying above a fixed distance r_c

$$K_{ij} = \theta(r_c - |\vec{r}_{i0} - \vec{r}_{j0}|)$$

The residues of the proteins are divided in surface and bulk residues. The latter ones are determined by calculating the surface portion accessible at each site to the solvent and assigning to the bulk the residues whose exposed surface was less than a fixed value of 80 Å^2. This procedure assigned 249 residues out of 741 to the surface, which corresponds to a surface fraction $f = 0.336$ (see Eq. (40)). Here the surface fraction vector is simply taken as

$$S_i = \begin{cases} 0 & i \in \text{bulk} \\ 1 & i \in \text{surface} \end{cases}$$

We perform a cooling experiment in the usual fashion: the protein is first equilibrated at constant energy so that each linear mode is given approximately an energy of β^{-1} at the

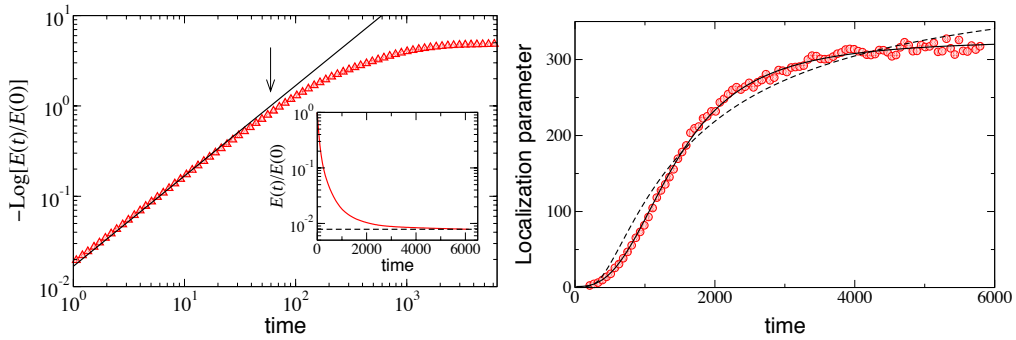

(a) (b)

Figure 19: (a) Energy decay in Citrate Synthase with FPU springs connecting nearest neighbouring residues. The solid line is a plot of the exponential law $E(t)/E(0) = \exp(-t/\tau_0)$. The dashed line in the inset marks the asymptotic energy left in the protein $E(\infty) \approx 18.7$. The vertical arrow shows the expected crossover time $\tau_0 = 1/f\zeta \approx 59.5$. (b) Plot of the localization parameter (symbols). The dashed line is the best fit with Eq. (48). The solid line is the best fit obtained with formula (55), with $t_0 = 1430$, $\sigma = 2.85$ and $\mathcal{L}_\infty = 324.1$. Parameters are $\zeta = 0.05$, $N = 741$, $f = 0.336$, $E(0)/N = 3.21$

end of the equilibration stage, and then the dissipative dynamics is started by integrating the equations of motion

$$m_i \ddot{\vec{r}}_i = -\sum_{j=1}^{N} \theta(r_c - |\vec{r}_{i0} - \vec{r}_{j0}|) \frac{\partial U(\{\vec{r}_j\})}{\partial \vec{r}_i} - m_i \sum_{j=1}^{N} \Gamma_{ij} \dot{\vec{r}}_j \tag{54}$$

where $\Gamma_{ij} = \zeta S_i \delta_{ij}$ is the damping matrix, that controls the flow of energy to the environment through the protein surface.

In Fig. 19 (a) we plot the total energy relaxation of one realization of initial energy $E(0)/N = 3.21$. The first stage is an exponential decay with time constant given by the same formula as for the harmonic chain, i.e. $\tau_0 = 1/f\zeta$. We have already seen that this as the case in the relaxation of a protein described within the harmonic approximation of its associated elastic network. We see now that the same description applies to the first stage of relaxation dynamics within the framework of a full network of nonlinear FPU springs, in the same way as the mathematical description of the harmonic chain may be extended to an FPU chain. Henceforth, in accordance with the same picture, a crossover is observed also here at a time of the order of $1/f\zeta \approx 59.5$, that marks the onset of localization and the corresponding slowing down of the energy flow until a pseudo-stationary state is attained. During this last stage, a nonlinear excitation has self-localized at one site of the structure. Due to the strong similarities with what is observed in regular nonlinear lattices, we shall call it discrete breather. The localization is evident from the curve of the localization parameter (46), shown in Fig.19 (b). In this case, the guess (48) seems not to capture satisfactorily the numerical data. Instead, the empirical function already used in the case of

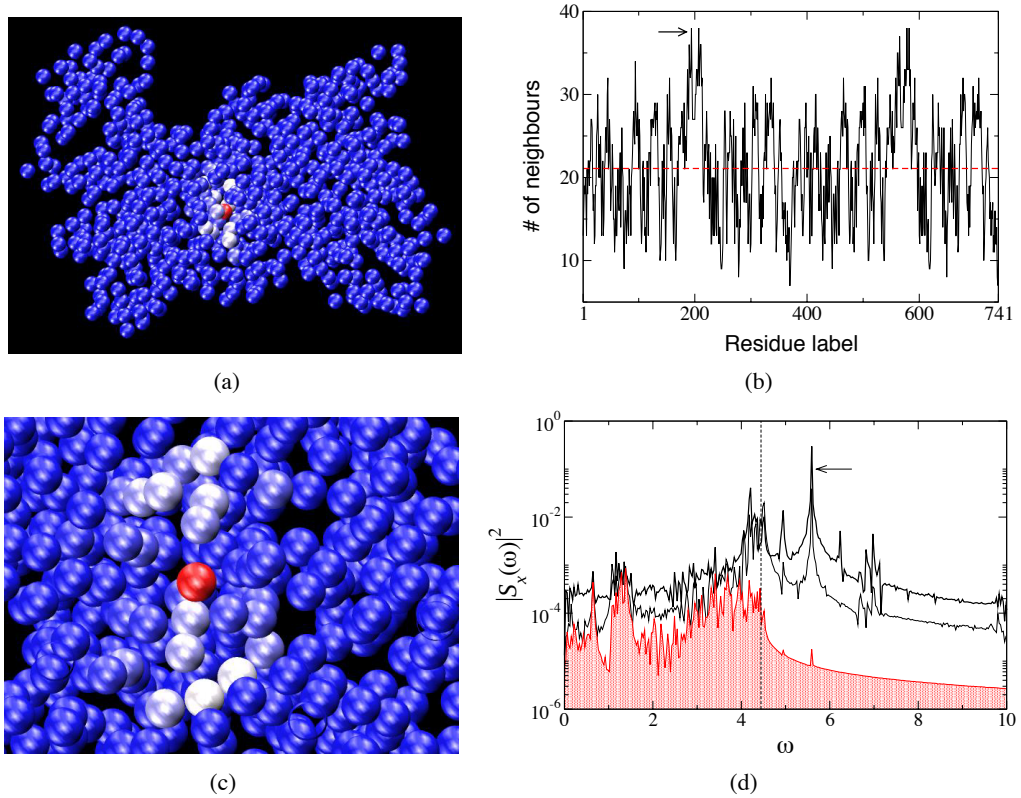

Figure 20: (a) Cartoon of the coarse-grained model of Citrate Synthase structure in the pseudo-stationary state. Each sphere represents the position of the $\alpha-$carbon of an amino-acid. The residues are color-coded according to their energy. (b) Plot of residue connectivities (number of neighbours). The connectivity of the $i-$th amino-acid is defined as $\sum_j \theta(r_c - |\vec{r}_{i0} - \vec{r}_{j0}|)$. The solid line marks the average protein connectivity. The arrow signals the high connectivity of the residue Threonine 206, where the breather eventually localizes. (c) Close up of the Citrate Synthase structure in the pseudo-stationary state in the region where the breather has self-localized. (d) Power spectrum of displacements of the central particle of the breather (thick solid line), its neighbour within the breather (thin solid line), and a third particle chosen faraway from the breather in the protein structure. The arrow marks the principal nonlinear component of vibration. The dashed vertical line marks the edge of the linear spectrum at $\omega_0 = 4.4448$. Parameters are: $\zeta = 0.05$, $N = 741$, $f = 0.336$, $E(0)/N = 3.21$, $r_c = 10$ Å.

a two-dimensional FPU lattice shows to provide an excellent interpolation, that is

$$\mathcal{L}(t) = \frac{\mathcal{L}_\infty \left(\frac{t}{t_0}\right)^\sigma + \mathcal{L}_0}{\left(\frac{t}{t_0}\right)^\sigma + 1} \tag{55}$$

In this way, a localization time $t_0 \simeq 1430$ can be extracted from the numerical curve, that is a time span that covers about 10^3 periods of the bande-edge mode.

By the time the system has reached its pseudo-stationary state, the localized mode has gathered about six times the initial energy density, as it shows in Fig. 19 (a) and appears to have a localization length of the order of $10\,\text{Å}$, i.e. of the same order of the value chosen as cutoff for determining interacting pairs. The breather localizes the greatest portion of its energy onto a central particle (corresponding to the residue Threonine 206) and onto a few of its neighbours, with an amplitude that decreases exponentially from the center (see Fig. 20 (a),(c)). That the breather is indeed a localized mode of nonlinear origin can be clearly appreciated by looking at the power spectrum of displacements of the particles within its localization length calculated in a time window within the pseudo-statonary state. The main nonlinear component is manifest in Fig. 20 (d), where the power spectrum of a particle lying faraway from the breather center is also reported, showing spectral power only in the interval corresponding to the linear spectrum.

One striking feature of the breather that emerges in protein structures such as Citrate Synthase is what we may call *selective localization*. As a matter of fact, for a given value of the initial energy and of the interaction cutoff r_c, i.e. of the overall *tightness* of the structure, one seems either to observe a breather developing or not. If the breather does form, it will be in a region characterized by a high degree of local connectivity (see Fig. 20 (b)). This can be also understood by recalling that breathers in the context of surface cooling are expected to detach from the edge of the linear band. However, while the corresponding (unstable) modes are extended in regular lattices (e.g. the π mode), in a protein structure the patterns of bande-edge modes are strongly localized. As a matter of fact, the mode with the highest frequency in Citrate Synthase appears to be localized in the same region where the breather self-excites. This remarkable fact also helps explaining why not all protein structures allow for the self-localization process at a given value of the interaction cutoff[2]. If the residue displacements within the mode involve particles that belong to the surface, there is a strong chance that the energy stored in the mode will be too soon drained, thus suppressing fluctuations with the good frequencies for triggering the localization process. Incidentally, the phenomenon of selective localization in proteins indirectly provides further support for the cause of modulational instability as the driving mechanism of self-localization.

4 Conclusions and perspectives

In this paper I have presented a rather rich, although somewhat heterogeneous survey of phenomena related to the extraction of energy through the surface in systems whose size allows for a sizable surface/bulk ratio. I shall here briefly retrace the *fil rouge* that led us through all the material in order to highlight the important points and at the same time state more clearly the exciting perspectives that remain open.

The first important point is the following. An extended system that is allowed to exchange energy through its surface with its environment is characterized by an extended

[2]The process of spontaneous energence of breathers can be tuned by also acting on the parameter r_c, that regulates the overall rigidity of the structure and hence also affects the spatial patterns of normal modes. Hence, the comparison among different protein structures is only meaningful here at fixed values of r_c.

spectrum of relaxation rates, each controlling the exponential channelling of energy of a given elementary vibrational mode. This effect is a direct result of the anisotropy of coupling to the exterior, which automatically selects a bulk and a non-vanishing surface.

The second important point is that cooling a nonlinear system from the surface leads to spontaneous pinning of energy in the form of self-excited localized vibrations. Remarkably, this seems to be a fairly common phenomenon, that manifests itself irrespective of the specific type of nonlinearity characterizing the potential energy. What is also important, the signature of the spontaneous energy focussing on the temporal behaviour of global observables such as the total energy can be extremely subtle to decipher. In fact, an accurate analysis of the natural term of comparison for the behaviour of such quantities, i.e. the same system where the equations of motion have been linearized, led us to learn that even in this simple case one deals with non-trivial features. An intriguing example is provided by the FPU chain, whose total energy indeed attains a pseudo-stationary state in the long run, where energy is very efficiently pinned at a few sites and stays localized virtually forever. However, if one looks carefully at the time behaviour of the portion of decay during the process of localization, hardly no differences can be remarked with respect to a simple chain of beads and Hookean springs. What should be kept in mind is that it is profoundly misleading to speak of "slow relaxation" as a direct signature of the emergence of localized objects. In fact, as we have seen, the simplest system of all under edge cooling releases its energy following a power law of the type $t^{-d/2}$. In one dimension we have seen that this observation can be rationalized in the framework of macroscopic diffusion of heat.

One might think, as it was suggested in the beginning, that stretched exponential relaxation would be a more distinctive feature of the emergence of localized vibrations. This would be important for example in trying to identify such process experimentally, where one has most easily access to global observables. However, we have seen that the presence of spatial disorder, be it the intricate topology of a protein or the surface/bulk mismatch of a nano-crystal, indeed suffices to force energy to decay following a stretched exponential. As we have learnt from the FPU case, that is not a necessary condition for localization to be present. With the analysis of disordered harmonic systems, we have also demonstrated that it is not even a sufficient condition for self-localization.

Now we come to the most fascinating point of the history. Of course, the nature of the objects that self-localize under edge cooling will be different and subtly dependent on the details of the nonlinearities present in the inter-particle potential. Nonetheless, we have seen that there exist intriguing similarities between the characteristics of the localized modes and exact solutions with the same properties that are found in the Hamiltonian dynamics of the very same systems. I have concentrated the discussion of this point in the context of one- and two-dimensional FPU lattices, where the similarities with discrete breathers is striking. In that case, the whole process closely resembles the phenomenology of modulational instability of band-edge waves occurring in the absence of damping. Indeed, in ref. [25] we can find a first indirect confirmation that the damped system supports breathers similar to those known from the Hamiltonian case. The authors calculate a pattern corresponding to a zero-velocity DB solution numerically within the framework of the rotating wave ap-

proximation [73, 74] and then use such solution as the initial condition for the dissipative dynamics. What is observed is that the solution radiates away a tiny part of its initial energy through the boundaries thus stabilizing in a state identical to that obtained from a generical equilibrium initial condition. Of course, a more complete analysis of these aspects would be crucial. Not only in the case of FPU but also for other systems, such as the case of rotators that I have been briefly discussing here or other systems not even yet explored.

The picture that emerges overall is a fascinating one. In particular one whose implications might be vast if the generality that seems to characterize these phenomena is confirmed and made more quantitative. We may speculate that surface cooling in nonlinear systems could be a method for selecting specific, *typical* quasi-periodic orbits in the phase space by forcing a system to channel energy out through its surface. In other words, that would be tantamount to let the system exploit in a *clever* way its spontaneous energy fluctuations in order to excite specific solutions of the Hamiltonian dynamics. By pushing our wishful thinking further, we may also think of these phenomena as providing the rationale to *control* a system in such a way to lead it toward solutions specified *beforehand*.

That the impact of all this may be important also from an experimental point of view is magnificently demonstrated by a recent article by R. Livi, R. Franzosi and G.-L. Oppo [24]. In this paper, the authors study theoretically the dissipative dynamics of a Bose-Einstein condensate (BEC) trapped in an optical lattice and cooled trough the boundaries by removing atoms from the ends of the optical lattice. By approximating the condensate order parameter with a sum of Wannier functions in the tight-binding approximation, they end up studying the dynamics of a nonlinear one-dimensional extended system subject to edge cooling. Numerical integration of the equations of motion shows that localized states emerge in the system. What is most interesting, the authors succeed in comparing one of the asymptotic states that typically self-excite with a localized solution known to exist in the conservative system. Remarkably, they do not find any differences within their numerical level of accuracy. This study strongly suggests that edge cooling might be an extremely rich process to study in many contexts of non-equilibrium statistical physics. Moreover, the actual possibility of experimentally realizing such a setup for obtaining localized BECs, as outlined by the authors in the paper, may pave the way for a wider experimental verification of such intriguing phenomenology. In the authors' words:

> Self-localization due to boundary dissipations is a universal phenomenon and should be observable under general conditions of operation of BEC in optical lattices as well as other experimental realizations. [. . .] Beyond its practical interest for BEC and Optics, the boundary cooling technique has an intrinsic conceptual interest. In fact, it allows to perform a low-energy limit which selects naturally, by exploiting the statistics of energy fluctuations [. . .], genuine nonlinear quantum states in the form of long-lived periodic (static or moving) localized solutions.

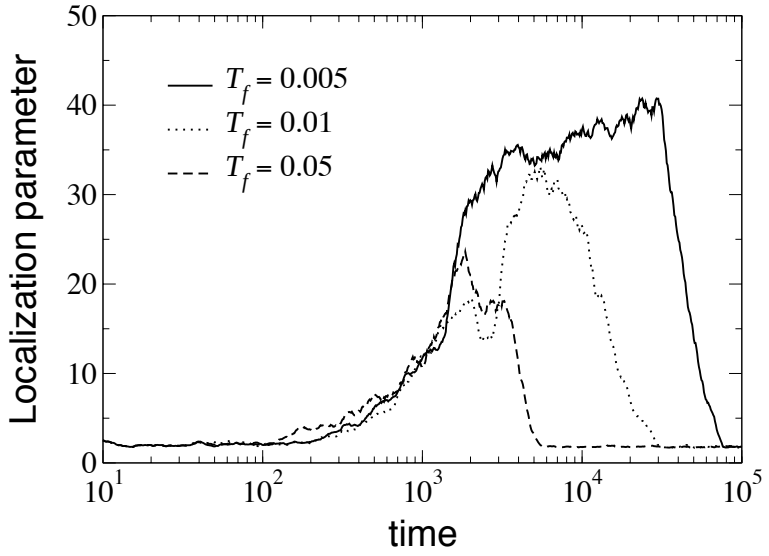

Figure 21: Plot of the localization parameter for an FPU chain relaxing from a temperature $T_i = 5$ to different final temperatures. Parameters are: $\eta = 1$, $m = 1$, $N = 100$.

4.1 Open problems: breathers in a thermal environment

What exactly should be called a breather when a system is not at constant energy is an extremely subtle matter [75]. Typically, at high temperatures, i.e. when strong anharmonicities are present, one observes *hot spots* of vibrational energy [76]. These localized energy fluctuations usually persist for times order of magnitude greater than the normal modes of the system and are thus loosely termed breathers [77–80]. However, it is not clear how long should be a long-lasting fluctuation in the high anharmonicity regime, and a rigorous analysis of the distribution of energy fluctuations at equilibrium in such contexts is still lacking. The scheme presented in this review nicely lends itself to explore the effects of a thermal bath on breathers' lifetime. Here, we just want to *throw the stone*, so as to stress once more the importance of further work in this direction.

Let us come back to the one-dimensional FPU chain. Instead of performing a relaxation experiment from a fixed temperature to zero temperature, we now want to study the relaxation of the system from a temperature T_i to a finite temperature $T_f < T_i$. In order to do this, we replace Eqs. (47) with the following ones

$$\begin{aligned} m\ddot{u}_p &= V'(u_{p+1} - u_p) - V'(u_p - u_{p-1}) \quad p = 2, 3, \ldots, N-1 \\ m\ddot{u}_1 &= V'(u_2 - u_1) - m\zeta\dot{u}_1 + \xi_1 \\ m\ddot{u}_N &= -V'(u_N - u_{N-1}) - m\zeta\dot{u}_N + \xi_N \end{aligned} \tag{56}$$

where we have now added fluctuating forces at the surface satisfying the following proper-

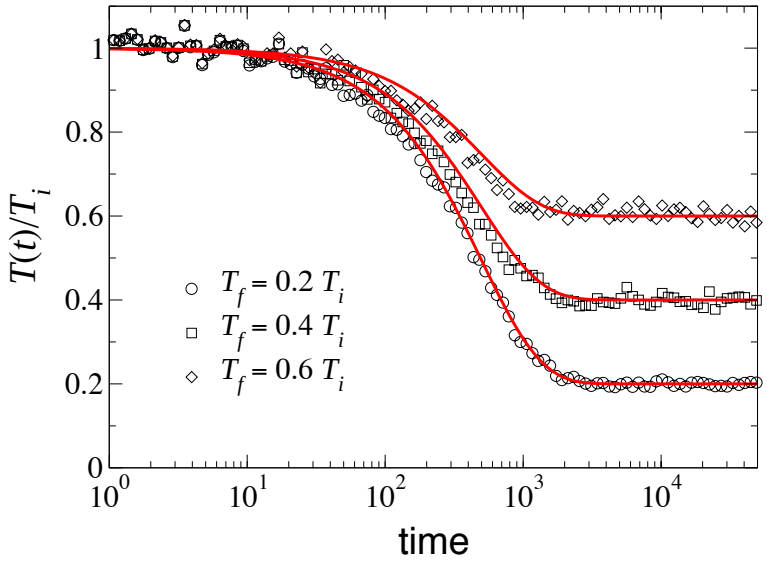

Figure 22: Plot of the (kinetic) temperature decay in a FPU chain relaxing from an initial temperature $T_i = 2$ to a specified fraction of its initial temperature. The data are averages over 20 initial conditions. Parameters are: $\eta = 0.1$, $m = 1$, $N = 100$. The solid lines are plots of formula (58).

ties[3]

$$\begin{aligned} &\langle \xi_i(t) \rangle = 0 \\ &\langle \xi_i(t)\xi_j(t') \rangle = 2k_B T_f m\zeta\delta_{i,j}\delta(t-t') \quad . \end{aligned} \tag{57}$$

In Fig. 21 we clearly see that even a small finite value of the asymptotic temperature T_f suffices to largely hinder the spontaneous localization process. In particular, it seems that when the energy left in the system becomes of the order of the work performed by the external random forces, the localization process breaks down and the energy is abruptly dispersed away through the boundaries. Hence, it seems that even a small amount of random external forces is enough for destabilizing the nonlinear modes that try to self-localize in the system.

In Fig. 22 we show the temporal behaviour of the temperature averaged over many initial conditions in a situation where the final temperature is so high as to make virtually impossible any attempt to self-localization. Surprisingly, the time scale controlling the exchange of energy with the environment, namely the damping rate η, seems here to explain the observed trend. In fact, the numerics shows to be very well interpolated by the single exponential

$$T(t) = (T_i - T_f)e^{-t/\tau_0} + T_f \tag{58}$$

where $\tau_0 = N/2\eta$. In fact, this was somewhat expected, since we already know that the

[3]We stress that the choice of a Langevin thermostat for realizing the thermal bath at the boundaries is arbitrary and the results presented here might well depend on the particular realization of the temperature reservoirs.

time scale τ_0 controls the first, major energy drop during a relaxation through the surface. More precisely, with a very accurate statistics and in the case of a drop to extremely small temperatures, we expect that the crossover to a power law should be observable. Once more, we see that in the absence of localization the behaviour of an harmonic chain offers an excellent interpretation frame for the behaviour of the FPU chain.

Concluding, we have presented evidence that spontaneous localization emerging from energy relaxation across the surface is hindered in the presence of a thermal bath keeping a finite temperature at the interface. In this case, the preliminar phenomenology seems to indicate that the region of parameter space where nonlinear modes self-localize is substantially reduced. Moreover, the latter are in this case characterized by finite lifetimes that depend on both the initial and final temperatures.

Acknowledgments

First and foremost I would like to thank Stefano Lepri and Roberto Livi, who contributed substantially to the material presented here as my coauthors in the past years. I am also grateful to Yves-Henri Sanejouand and Brice Juanico for stimulating discussions and for letting me anticipate some of the latest results on nonlinear dynamics of proteins. Finally, I wish to express my gratitude to Paolo De Los Rios, for his many insightful comments and remarks during our numerous discussions.

A

In this Appendix we report the details of the calculation of the damping rates for the harmonic lattice in the underdamped regime $\eta \ll 1$. The eigenvectors of the Hamiltonian problem satisfy the orthonormality conditions

$$\begin{aligned}(\psi^\alpha, \psi^{\alpha\,\prime}) &= \sum_{p=0}^{N-1} \psi_p^\alpha \psi_p^{\alpha\,\prime} = \delta_{\alpha,\alpha\,\prime} \\ (\psi^\alpha, K\psi^{\alpha\,\prime}) &= \sum_{p,p\,\prime=0}^{N-1} \psi_p^\alpha K_{pp\,\prime} \psi_{p\,\prime}^{\alpha\,\prime} = -\omega_\alpha^2 \delta_{\alpha,\alpha\,\prime},\end{aligned} \tag{59}$$

By substituting expression (5) in equation (2), we get

$$\sum_{\alpha=0}^{N-1} [\ddot{c}_\alpha(t) - \omega_\alpha^2 c_\alpha(t) - 2i\omega_\alpha \dot{c}_\alpha(t)] e^{-i\omega_\alpha t} \psi_p^\alpha - \sum_{\alpha=0}^{N-1} c_\alpha(t) e^{-i\omega_\alpha t} \sum_{p\,\prime=0}^{N-1} K_{pp\,\prime} \psi_{p\,\prime}^\alpha = - \sum_{\alpha=0}^{N-1} [\dot{c}_\alpha(t) - i\omega_\alpha c_\alpha(t)] e^{-i\omega_\alpha t} \sum_{p\,\prime=0}^{N-1} \Gamma_{pp\,\prime} \psi_{p\,\prime}^\alpha.$$

By taking the scalar product of the latter equation with $\psi^{\alpha\,\prime}$ and recalling the orthonormality conditions contained in (59), we are led to the system of equations

$$\ddot{c}_\alpha(t) - 2i\omega_\alpha \dot{c}_\alpha(t) = -\sum_{\alpha\,\prime=0}^{N-1} \left[\dot{c}_{\alpha\,\prime}(t) - i\omega_{\alpha\,\prime} c_{\alpha\,\prime}(t)\right] \Gamma^{\alpha\alpha\,\prime} e^{-i(\omega_{\alpha\,\prime}-\omega_\alpha)t}, \tag{60}$$

where

$$\Gamma^{\alpha\alpha\,\prime} = (\psi^\alpha, \Gamma\, \psi^{\alpha\,\prime}) = \sum_{p,p\,\prime=0}^{N-1} \psi_p^\alpha \Gamma_{pp\,\prime} \psi_{p\,\prime}^{\alpha\,\prime} \tag{61}$$

We can obtain approximate solutions of system (60) by means of a perturbative series of the form

$$c_\alpha(0) = c_\alpha^{[0]}(t) + c_\alpha^{[1]}(t) + c_\alpha^{[2]}(t) + \ldots,$$

where $c_\alpha^{[1]}(t), c_\alpha^{[2]}(t), \ldots$ are first order, second order amplitudes, and so on, in the perturbation parameter η. We can then use the usual iterative procedure. If we assume that at $t = 0$ only the mode $\alpha = \bar{\alpha}$ is populated, we can approximate $c_\alpha(t) = \delta_{\alpha,\bar{\alpha}}$ (independent of t) in the right–hand side of equation (60) and then integrate to get $c_\alpha^{[1]}(t)$. The procedure can be repeated for obtaining $c_\alpha^{[2]}(t)$, etc. For the first order approximation we obtain the following equation

$$\ddot{c}_\alpha(t) - [2i\omega_\alpha - \Gamma^{\alpha\alpha}]\dot{c}_\alpha(t) - i\omega_\alpha \Gamma^{\alpha\alpha} c_\alpha(t) = 0,$$

which is readily integrated, yielding expression (6).

To calculate the matrix elements $\Gamma^{\alpha\alpha}$, we need the explicit expression of the eigenvectors of the unperturbed problem, which are

$$\begin{aligned} \psi_p^\alpha &= \sqrt{\tfrac{2}{N}} \cos\left[q_\alpha \left(p + \tfrac{1}{2}\right)\right] \qquad \ldots \quad \text{Free ends BC} \\ \psi_p^\alpha &= \sqrt{\tfrac{2}{N}} \sin\left[q_\alpha \left(p + 1\right)\right] \qquad \ldots \quad \text{Fixed ends BC} \end{aligned} \tag{62}$$

where

$$\begin{aligned} q_\alpha &= \frac{\alpha\pi}{N} \qquad\qquad \ldots \quad \text{Free ends BC} \\ q_\alpha &= \frac{(\alpha+1)\pi}{N+1} \qquad \ldots \quad \text{Fixed ends BC} \quad . \end{aligned}$$

with $\alpha = 0, 1 \ldots N-1$. By inserting expressions (62) into the matrix elements (61), one can easily obtain equations (7).

B

In this appendix we report the details of the solution of the heat equation with the initial conditions (12)

$$T(x,0) = \begin{cases} T_i & \text{for} \quad |x| < \ell \qquad \text{(region 1)} \\ T_f & \text{for} \quad |x| > \ell \qquad \text{(region 2)} \end{cases} \tag{63}$$

with $T_i > T_f$. The x axis is divided into regions 1 and 2, characterized by the thermal conductivities κ_m and thermal diffusion coefficients D_m, $m = 1, 2$. Given the symmetry of the problem, we can restrict the calculation of the temperature profile to the positive semi-axis. Consequently, the problem can be formulated in the form of a system of heat equations

$$\begin{cases} \dfrac{\partial T_1(x,t)}{\partial t} = D_1 \dfrac{\partial^2 T_1(x,t)}{\partial x^2} & 0 \le x < \ell \\ \dfrac{\partial T_2(x,t)}{\partial t} = D_2 \dfrac{\partial^2 T_2(x,t)}{\partial x^2} & x \ge \ell \end{cases} \tag{64}$$

where we have defined the two temperature profiles $T_1(x,t)$ and $T_2(x,t)$ such as

$$T(x,t) = \begin{cases} T_1(x,t) & 0 \le x < \ell \\ T_2(x,t) & x \ge \ell \end{cases} \tag{65}$$

The complete set of boundary conditions may be specified as follows:

- **Continuity of the temperature field**

$$\lim_{x \to \ell^-} T_1(x,t) = \lim_{x \to \ell^+} T_2(x,t) \tag{66a}$$

- **Continuity of the the heat flux**

$$\lim_{x \to \ell^-} \kappa_1 \frac{\partial T_1(x,t)}{\partial x} = \lim_{x \to \ell^+} \kappa_2 \frac{\partial T_2(x,t)}{\partial x} \tag{66b}$$

- **Absence of heat sources**

$$\lim_{x \to \infty} T_2(x,t) = 0 \tag{66c}$$

- **Symmetry at** $x = 0$

$$\lim_{x \to 0^+} \frac{\partial T_1(x,t)}{\partial x} = 0 \tag{66d}$$

It is simpler to work with the reduced temperature profiles, we then perform the following substitution

$$\begin{aligned} \theta_1(x,t) &= T_1(x,t) - T_f \\ \theta_2(x,t) &= T_2(x,t) - T_f \end{aligned} \tag{67}$$

where now

$$\theta(x,0) = \begin{cases} \Delta T & \text{for} \quad 0 \le x < \ell \\ 0 & \text{for} \quad x \ge \ell \end{cases} \tag{68}$$

with $\Delta T = T_i - T_f$.

Let us introduce the Laplace transform of the reduced temperature profiles

$$\bar{\theta}_m(x,s) = \int_0^\infty e^{-st} \theta_m(x,t)\, dt \qquad m = 1, 2 \quad . \tag{69}$$

The Laplace transform of equations (64) then reads

$$\begin{cases} s\,\bar{\theta}_1(x,s) - \Delta T = D_1 \dfrac{\partial^2 \bar{\theta}_1(x,s)}{\partial x^2} & 0 \le x < \ell \\ s\,\bar{\theta}_2(x,s) = D_2 \dfrac{\partial^2 \bar{\theta}_2(x,s)}{\partial x^2} & x \ge \ell \end{cases} \tag{70}$$

The general solution of system (70) reads

$$\begin{cases} \bar{\theta}_1(x,s) = \dfrac{\Delta T}{s} + A e^{\sqrt{s\tau_1}(x/\ell)} + B e^{-\sqrt{s\tau_1}(x/\ell)} & 0 \le x < \ell \\ \bar{\theta}_2(x,s) = C e^{\sqrt{s\tau_2}(x/\ell)} + D e^{-\sqrt{s\tau_2}(x/\ell)} & x \ge \ell \end{cases} \tag{71}$$

where A, B, C, D are constants and we have introduced the thermal time scales $\tau_m = \ell^2/D_m, m = 1, 2$. Applying the boundary conditions (66c) and (66d), we get, respectively,

$$A = B \quad \text{and} \quad C = 0$$

so that

$$\begin{cases} \bar{\theta}_1(x,s) = \dfrac{\Delta T}{s} + 2A \cosh[\sqrt{s\tau_1}(x/\ell)] & 0 \le x < \ell \\ \bar{\theta}_2(x,s) = D e^{-\sqrt{s\tau_2}(x/\ell)} & x \ge \ell \end{cases} \tag{72}$$

If we now impose the boundary conditions (66a) and (66b), we get

$$\begin{cases} 2A \cosh[\sqrt{s\tau_1}] + \dfrac{\Delta T}{s} = D e^{-\sqrt{s\tau_2}} \\ 2A \sinh[\sqrt{s\tau_1}] = -\mathbb{K} D e^{-\sqrt{s\tau_2}} \end{cases} \tag{73}$$

where we have introduced the relative heat strength defined in Eq. (16)

$$\mathbb{K} = \frac{\kappa_2}{\kappa_1}\sqrt{\frac{D_1}{D_2}}$$

Solving system (73) we determine the constants A and D. Substituting back into expressions (72), we finally get

$$\begin{cases} \bar{\theta}_1(x,s) = \dfrac{\Delta T}{s}\left\{1 - \dfrac{\mathbb{K}\cosh[\sqrt{s\tau_1}(x/\ell)]}{\mathbb{K}\cosh[\sqrt{s\tau_1}] + \sinh[\sqrt{s\tau_1}]}\right\} & 0 \le x < \ell \\ \bar{\theta}_2(x,s) = \dfrac{\Delta T}{s} \dfrac{e^{\sqrt{s\tau_2}(1-x/\ell)}\sinh[\sqrt{s\tau_1}]}{\mathbb{K}\cosh[\sqrt{s\tau_1}] + \sinh[\sqrt{s\tau_1}]} & x \ge \ell \end{cases} \tag{74}$$

In order to invert the Laplace transforms (74), we must compute the following integrals

$$\theta_m(x,t) = \frac{1}{2\pi i}\int_{\delta - i\infty}^{\delta + i\infty} \bar{\theta}_m(x,s)\, e^{st}\, ds \qquad m = 1, 2 \tag{75}$$

where δ must be chosen as usual so that all singularities of the functions $\bar{\theta}_m(x,s)$ lie in the portion of the complex plane to the left of the straight line $\Re(s) = \delta$. We see that the transforms (74) contain $\sqrt{s}$, which is a multi-valued complex function with a branch cut

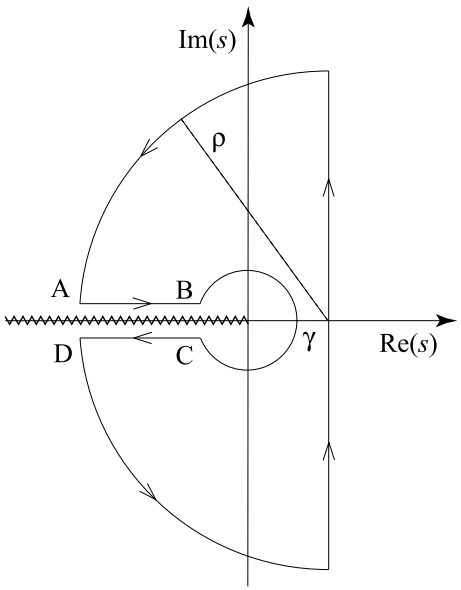

Figure 23: Closed contour Γ in the complex plane used for evaluating the integral (75).

on the real axis. Moreover, they have a simple pole at the origin. Hence, we use standard contour deformation as sketched in Fig. 23. From the Cauchy theorem it follows that

$$\frac{1}{2\pi i}\oint_{\Gamma}\bar{\theta}_m(x,s)e^{st}\,ds=0 \qquad m=1,2$$

In particular, we may decompose the integral on the closed contour Γ in the following fashion (see Fig. 23)

$$\oint_{\Gamma}\cdots=\int_{C_\rho}\cdots+\int_{\gamma}\cdots+\int_{-\infty|AB}^{0}\cdots+\int_{0|CD}^{\infty}\cdots+\int_{\eta}\cdots$$

where C_ρ is the semicircle of radius ρ and center on the real axis in δ, γ is a circle of vanishing radius with center in the origin and η is the vertical line $\Re(s)=\delta$. By taking the limit for $\rho\to\infty$, we have $(m=1,2)$

- $\displaystyle\int_{\eta}\bar{\theta}_m(x,s)\,e^{st}\,ds=\theta_m(x,t)$
- $\displaystyle\int_{C_\rho}\bar{\theta}_m(x,s)\,e^{st}\,ds=0$ by virtue of Jordan's Lemma, since

$$\lim_{\rho\to\infty}\left|s\,\bar{\theta}_m(x,s)\,e^{st}\right|_{C_\rho}=0$$

- $\displaystyle\int_{\gamma}\bar{\theta}_m(x,s)\,e^{st}\,ds=-\mathrm{Res}[\bar{\theta}_m(x,s)\,e^{st}]_{s=0}$ the minus sign arising because the circle γ is followed clock-wise.

Moreover, if $s = re^{i\varphi}$, because of the branch cut we have

$$s|_{AB} = re^{i\pi}$$
$$s|_{CD} = re^{-i\pi}$$

By putting everything together, we finally get

$$\begin{aligned}\theta_m(x,t) = \frac{1}{2\pi i}\int_0^\infty e^{-rt}\left[\bar{\theta}_m(x,s)|_{s=re^{-i\pi}} - \bar{\theta}_m(x,s)|_{s=re^{i\pi}}\right] dr \\ + \text{Res}[\bar{\theta}_m(x,s)\, e^{st}]_{s=0}\end{aligned} \tag{76}$$

Substituting expressions (74) into Eq. (76), we get after some algebra the reduced temperature profile inside the initially hot region

$$\theta_1(x,t) = \frac{2\mathbb{K}\Delta T}{\pi}\int_0^\infty \frac{e^{-u^2(t/\tau_1)}}{u}\left\{\frac{\cos[u(x/\ell)]\sin u}{\mathbb{K}^2\cos^2 u + \sin^2 u}\right\} du \tag{77}$$

The explicit expression for $\theta_2(x,t)$ can be obtained with the same procedure. Hence, the average normalized reduced temperature of medium 1 can be readily calculated as

$$\begin{aligned}\langle\Theta_1(t)\rangle &= \frac{1}{\ell\Delta T}\int_0^\ell \theta_1(x,t)\, dx \\ &= \frac{2\mathbb{K}}{\pi}\int_0^\infty e^{-u^2(t/\tau_1)}\left(\frac{\sin u}{u}\right)^2 \frac{du}{\mathbb{K}^2\cos^2 u + \sin^2 u}\end{aligned} \tag{78}$$

For $\mathbb{K} = 1$, the integral (78) can be solved analytically (see main text). However, the long-time behaviour can be estimated with simple arguments. Let us perform the following change of variable

$$y = \sqrt{\frac{t}{\tau_1}}\, u \quad .$$

Now, for $t \gg \tau_1$, we have up to terms of $\mathcal{O}(\sqrt{\tau_1/t})$ in the integrand

$$\frac{\sin(y\sqrt{\tau_1/t})}{y\sqrt{\tau_1/t}} \simeq 1, \qquad \cos(y\sqrt{\tau_1/t}) \simeq 1, \qquad \sin(y\sqrt{\tau_1/t}) \simeq 0$$

so that

$$\langle\Theta_1(t)\rangle \simeq \frac{1}{\mathbb{K}\sqrt{\pi t/\tau_1}}$$

i.e. $\langle\Theta_1(t)\rangle \propto t^{-d/2}$, $d = 1$ being the spatial dimension.

References

[1] E. Roduner, *Chem. Soc. Rev.* **35**, 583 (2006).

[2] E. Tosatti and S. Prestipino, *Science* **289**(5479), 561 (2000).

[3] K. Kinbara and T. Aida, *Chem. Rev.* **105**, 1377 (2005).

[4] F. Piazza, P. De Los Rios and Y.-H. sanejouand, *Phys. Rev. Lett.* **94**, 145502 (2005).

[5] L. A. Amos and R. A. Cross, *Curr. Opin. Struct. Biol.* **7**, 239 (1997).

[6] J. A. Spudich, *Nature* **7**, 515 (1994).

[7] J. E. T. Corrie *et al.*, *Nature* **400**, 425 (1999).

[8] K. Kitamura, N. Tokunaga, S. Esaki, A. H. Iwane and T. Yanagida, *Curr. Biophysics (Japan)* **1**, 1 (2005).

[9] A. Xie, L. Van Der Meer and R. H. Austin, *J. Biol. Phys.*, **28**, 147 (2002).

[10] M. Hu and G. V. Hartland, *J. Phys. Chem. B*, **106**, 7029 (2002).

[11] G. P. Tsironis, S. Aubry, *Phys. Rev. Lett.* **77** (26) 5225 (1996).

[12] S. Flach, C.R. Willis, *Phys. Rep.*, **295**, 181 (1998).

[13] S. R. Bickham, S. A. Kiselev and A. J. Sievers, Phys. Rev. B **47**(21), 14206 (1993).
A. J. Sievers and S. Takeno, *Phys. Rev. Lett.* **6**(8), 970-973 (1988).

[14] A. Franchini, V. Bortolani, and R.F. Wallis,*J. of Phys.-Cond. Matter* **14**, 145 (2002).

[15] R. S. Mackay and S. Aubry, *Nonlinearity* **7**(6), 1623 (1994).
S. Aubry, *Physica D* **103**(1-4), 201 (1997).

[16] J. L. Marin and S. Aubry S *Physica D* **119**(1-2), 163 (1998).
J. L. Marin , S. Aubry and L. M. Floria, *Physica D* **113**(2-4), 283 (1998).

[17] D. Bambusi, *Nonlinearity* **9**(2), 433 (1996).

[18] M. Schuster, F. Pignatelli, A. V. Ustinov, *Phys. Rev. B* **69** (9), 094507 (2004).

[19] P. Binder, A. V. Ustinov, *Phys. Rev. E* **66** (1), 016603 Part 2 (2002).

[20] M. Sato, B. E. Hubbard, A. J. Sievers, B. Ilic, D. A. Czaplewski, H. G. Craighead, *Phys. Rev. Lett.* **90**(4), art. no. 044102 (2003).

[21] U. T. Schwarz, L. Q. English, and A. J. Sievers, *Phys. Rev. Lett.*, **83**(1) 223 (1999).

[22] T. Rossler and J. B. Page, *Phys. Rev. B*, **62**(17), 11460 (2000).

[23] D. Bonart and J. B. Page, *Phys. Rev. E* **60** (2) R1134-R1137 (1999).

[24] R. Livi, R. Franzosi, and G.-L. Oppo, *Phys. Rev. Lett.* **97**, 060401 (2006).

[25] F. Piazza, S. Lepri and R. Livi, *J. Phys. A*, **34**, 9803 (2001).

[26] F. Piazza, S. Lepri and R. Livi, *Chaos*, **13**(2), 637 (2003).

[27] M. Elefhteriou, S. Lepri, R. Livi and F. Piazza, *Physica D* **204**(3-4), 230 (2005).

[28] R. Reigada, A. Sarmiento and K. Lindenberg, *Phys. Rev. E*, **64**(4) 066608 (2001).

[29] R. Reigada, A. Sarmiento and K. Lindenberg, *Phys. Rev. E*, **66**(4) 046607 (2002).

[30] I. Daumont T. Dauxois and M. Peyrard, *Nonlinearity* **10**(3), 617 (1997).

[31] T. Dauxois, R. Khomeriki, F. Piazza and S. Ruffo *Chaos* **15**, 015110 (2005).

[32] H. Meyer-Ortmanns, P. T. Landsberg, S. Abe, A. K. Rajagopal and T. Yamano, *Ann. Phys. (Leipzig)* **11**, 457 (2002).

[33] F. Cooper *Int. J. Heat Mass Transfer*, **20**(9), 991 (1977).

[34] M. M. Tirion, *Phys. Rev. Lett.* **77**, 1905 (1996).

[35] T. Haliloglu, I. Bahar and B. Erman, *Phys. Rev. Lett.*, **79**, 3090 (1997).

[36] A. R. Atligan, S. R. Durrell, R. L. Jernigan, M. C. Demirel, O. Keskin and I. Bahar, *Biophys. J.*, **80**, 505 (2001).

[37] K. Hinsen, *Proteins*, **33**, 417 (1998).

[38] F. Tama and Y. H. Sanejouand, *Protein Engineering*, **14**, 1 (2001).

[39] G. Lamm and A. Szabo, *J. Chem. Phys.*, **85**(12), 7334 (1986).

[40] H. Risken, *The Fokker–Planck Equation*, Springer, New York (1984).

[41] A. Siber, *Phys. Rev.* B **70**, 075407 (2004).

[42] W. Hasel, T. F. Hendrickson and S. W. Clark, *Tetrahedron Comp. Method.*, **1**(2), 103 (1988). For Myoglobin I used the implementation provided by the Molecular Dynamics package CHARMM.

[43] S. Flach, C. R. Willis, *Physics Reports* **295**, 181 (1998).

[44] T. Dauxois, A. Litvak-Hinenzon, R. S. MacKay, A. Spanoudaki (Eds), *Energy Localisation and Transfer*, Advanced Series in Nonlinear Dynamics, World Scientific (2004).

[45] T. Cretegny, T. Dauxois, S. Ruffo, A. Torcini, *Physica D* **121**, 109 (1998).

[46] M. Eleftheriou and S. Flach, *Physica D* **202**, 142 (2005).

[47] E. Fermi, J. Pasta, S. Ulam, Los Alamos Science Laboratory Report No. LA-1940 (1955), unpublished; reprinted in Collected Papers of Enrico Fermi, edited by E. Segré (University of Chicago Press, Chicago, 1965), Vol. 2, p 978. also in *Nonlinear Wave Motion*, Newell A. C. Ed., Lecture in Applied Mathematics **15** (AMS, Providence, Rhode Island, 1974) and in *The Many-Body Problem*, Mattis C. C. Ed. (World Scientific, Singapore, 1993).

[48] J. L. Martin and S. Aubry, *Nonlinearity* **9**(6), 1501 (1996).

R. Livi, M. Spicci and R. S. MacKay *Nonlinearity* **10**(6), 1421 (1997).

G. James, *Comptes Rendus de l'Academie des Sciences, serie I-Mathematique*, **332**(6), 581 (2001).

B. Sanchez-Rey B, G. James J. Cuevas *et al.*, *Phys. Rev. B* **70**(1), 014301 (2004).

S. Flach and A. Gorbach, *Chaos* **1**(1), 015112 (2005).

[49] M.Pettini and M. Cerruti-Sola, *Phys. Rev. A* **44**, 975 (1991).

[50] N. J. Zabusky, M. D. Kruskal, *Phys. Rev. Lett.* **15**, 240 (1965).

T. Yu Astakhova and G. A. Vinogradov, *J. Phys. A* **39**, 3593 (2006).

[51] M. Kastner, *Phys. Rev. Lett.* **92**, 104301 (2004).

[52] S. Flach, K. Kladko, and R. S. MacKay, *Phys. Rev. Lett.* **78**, 1207 (1997).

[53] F. Piazza, S. Lepri and R. Livi, *Localisation as an activated process in 2D non–linear lattices*, Proceedings of the conference on Localization and Energy Transfer in Nonlinear Systems, June 17-21, 2002, San Lorenzo de El Escorial, Madrid, Spain, World Scientific (2002).

[54] A. V. Savin, O. V. Gendel'man, *Phys. Sol. State* **43** 355 (2001).

[55] S. Takeno and M. Peyrard, *Physica D* **92**, 140 (1996).

[56] S. Takeno and M. Peyrard, *Phys. Rev. E* **55**, 1922 (1997).

[57] S. Lepri, R. Livi and A. Politi, *Phys. Rep.* **377**, 1 (2003).

[58] C. Giardinà, R. Livi, A. Politi and M. Vassalli, *Phys. Rev. Lett.* **84**, 2144 (2000).

O. V. Gendel'man and A. V. Savin, *Phys. Rev. Lett.* **84**, 2381 (2000).

[59] S. Komineas, A. R. Bishop, F. G. Mertens, *Europhys. Lett.* **61**, 389 (2003).

[60] A.E. Sitnitsky, Invited contribution for the collection "Soft condensed matter. New research." Ed. F. Columbus, Nova Science Publishers, Inc., 2005.

[61] Peyrard, M. ed. "Nonlinear excitations is biomolecules"; Springer: Berlin, 1995.

[62] J. J. Falke, *Science* **295**(5559), 1480 (2002).

[63] D. Kern, E. Z. Eisenmesser and M. Wolf-Watz, *Enzyme Dynamics During Catalysis Measured by NMR Spectroscopy.* In: Thomas L. James, Editor(s), "Methods in Enzymology, Nuclear Magnetic Resonance of Biological Macromolecules", **394** 507-524, Academic Press (2005).

[64] K. Moritsugu, O. Miyashita and A. Kidera, *Phys. Rev. Lett.* **85**(18), 3970 (2000).

[65] A. V. Finkelstein, O. B. Pticyn, "Physics of protein" University press, Moscow, 2002.

[66] F. d'Ovidio, H. G. Bohr and P.-A. Lindgard, *J. Phys. C* **15** S1699 (2003).

[67] A. C. Scott, *Phys. Rep.* **217**, 1 (1992).

[68] D. M. Leitner, *J. Phys. Chem. A* **106**, 10870 (2002).
D. M. Leitner, *Phys. Rev. Lett.* **87**, 8102 (2001).

[69] S. Woutersen, P. Hamm, P. *J. Phys. C* **14**, R1035-R1062 (2002).

[70] A. Xie, A. van der Meer, W. Hoff and R.H.Austin, *Phys. Rev. Lett.* **84**, 5435 (2000).
A. Xie, A. van der Meer, W. Hoff and R.H.Austin, *Phys. Rev. Lett.* **88**, 018102 (2002).

[71] X. Yu, D. M. Leitner, *J. Phys. Chem. B* **107**, 1698 (2003).

[72] B. Juanico, F. Piazza, P. De Los Rios and Y.-H. Sanejouand, in preparation.

[73] A. J. Sievers and S. Takeno S *Phys. Rev. Lett.* **61**, 970 (1988).

[74] J. B. Page, *Phys. Rev. B* **41**, 7835 (1990).

[75] M. V. Ivanchenko, O. I. Kanakov, V. D. Shalfeev, and S. Flach, *Physica D* **198**, 120 (2004).

[76] S. Aubry, *Physica D* **103**, 201 (1997).

[77] T. Dauxois, M. Peyrard, and A. R. Bishop, *Phys. Rev. E* **47**, 684 (1993).

[78] K. O. Rasmussen, S. Aubry, A. R. Bishop, and G. P. Tsironis, *Eur. Phys. J. B* **15**, 169 (2000)

[79] G. Kalosakas, K. L. Ngai and S. Flach, *Phys. Rev. E*, **71**, 061901 (2005).

[80] M. Peyrard and J. Farago, *Physica A* **288**, 199 (2000).